



This is a repository copy of *On the use of linear-elastic local stresses to design load-carrying fillet-welded steel joints against static loading*.

White Rose Research Online URL for this paper:
<http://eprints.whiterose.ac.uk/90842/>

Version: Accepted Version

Article:

Ameri, A.A.H., Davison, J.B. and Susmel, L. (2015) On the use of linear-elastic local stresses to design load-carrying fillet-welded steel joints against static loading. *Engineering Fracture Mechanics*, 136. 38 - 57. ISSN 0013-7944

<https://doi.org/10.1016/j.engfracmech.2015.02.004>

Reuse

Unless indicated otherwise, fulltext items are protected by copyright with all rights reserved. The copyright exception in section 29 of the Copyright, Designs and Patents Act 1988 allows the making of a single copy solely for the purpose of non-commercial research or private study within the limits of fair dealing. The publisher or other rights-holder may allow further reproduction and re-use of this version - refer to the White Rose Research Online record for this item. Where records identify the publisher as the copyright holder, users can verify any specific terms of use on the publisher's website.

Takedown

If you consider content in White Rose Research Online to be in breach of UK law, please notify us by emailing eprints@whiterose.ac.uk including the URL of the record and the reason for the withdrawal request.



eprints@whiterose.ac.uk
<https://eprints.whiterose.ac.uk/>

Please, cite this paper as: Ameri, A. A. H., Davison, J. B., Susmel, L. On the use of linear-elastic local stresses to design load-carrying fillet-welded steel joints against static loading. *Engineering Fracture Mechanics*, 136, pp. 38-57, 2015.

On the use of linear-elastic local stresses to design load-carrying fillet-welded steel joints against static loading

A. A. H. Ameri, J. B. Davison and L. Susmel

Department of Civil and Structural Engineering, The University of Sheffield,
Sheffield S1 3JD, United Kingdom

Corresponding Author: Prof. Luca Susmel
Department of Civil and Structural Engineering
The University of Sheffield, Mappin Street, Sheffield, S1 3JD, UK
Telephone: +44 (0) 114 222 5073
Fax: +44 (0) 114 222 5700
e-mail: l.susmel@sheffield.ac.uk

ABSTRACT

This paper uses local linear-elastic stresses to estimate the static strength of steel arc welded joints. The proposed design methodology was developed by taking as a starting point the fundamental concepts on which the Theory of Critical Distances (TCD) is based. The overall accuracy of the devised approach was checked against a number of experimental results taken from the literature and generated by testing a variety of welded geometries. Such a systematic validation exercise demonstrated that the TCD is highly accurate in estimating the static strength of arc welded joints irrespective of the complexity of the assessed welded detail's geometry.

Keywords: Welded joints, design, static loading, Theory of Critical Distances.

INTRODUCTION

Reviews both in the USA and Europe [1, 2] indicate that in-service breakage of engineering structures and components costs around 4% of GNP in industrialised nations, the price which has to be paid becoming socially unacceptable whenever failures result in loss of human lives. In this complex scenario, one of the most difficult challenges faced by the metalworking sector is improving the in-service performance of structural assemblies by limiting not only the weight, but also the associated production, maintenance and energy costs.

With regard to the technological issues involved in the manufacturing process, it is well-known that a challenging aspect of making high-performance structures and components is efficiently joining

Please, cite this paper as: Ameri, A. A. H., Davison, J. B., Susmel, L. On the use of linear-elastic local stresses to design load-carrying fillet-welded steel joints against static loading. *Engineering Fracture Mechanics*, 136, pp. 38-57, 2015.

together the different parts. In this context, welding definitely represents the most widely used technological solution. In addition, welding plays a primary role in the repair and life extension of components and structures.

Although several welding technologies are used in manufacturing, arc welding is the most commonly adopted joining technology. As far as conventional arc welding is concerned, producing high quality weldments requires experienced welders capable of properly setting the necessary technological parameters. The overall quality of a weld mainly depends on the material microstructural features as well as on the geometry/size of the seams [3]. In particular, given the parent material, the most important technological variables affecting the quality of arc welded joints can be summarised as follows [4, 5]: preparation of the parent material, welding current, welding voltage, welding speed, shielding gas, metallurgical characteristics of the filler material and number/sequence of passes.

The above parameters are important also from a structural integrity point of view. In fact, the overall static strength of welded joints depends not only on the weld bead's geometrical features, but also on the microstructural features of the material in the vicinity of the seams themselves (especially the heat-affected zone) [6, 7]. Further, in conventional fillet welded joints subjected to uniaxial static loading, cracks are seen to initiate at the weld roots, subsequently propagating mainly through the weld beads [8]. This cracking behaviour suggests that, to efficiently control the overall strength of fillet arc welded joints, the technological variables must be set so that an adequate level of penetration can always be reached [9].

From a stress analysis point of view, if the parent and filler materials are assumed to obey a linear-elastic constitutive law, the stress fields in the vicinity of the weld roots are invariably singular [10], this holding true also in the presence of fabrication gaps [9]. In order to overcome the problem of handling singular stress fields without missing the undoubted advantages of linear-elastic stress analyses, existing design methods are based on the use of nominal stress quantities calculated with respect to a nominal weld throat area determined according to a variety of different geometrical rules [3, 11, 12]. Further, in order to correctly take into account the degree of multiaxiality of the applied systems of external forces and moments, the corresponding nominal stress components are

Please, cite this paper as: Ameri, A. A. H., Davison, J. B., Susmel, L. On the use of linear-elastic local stresses to design load-carrying fillet-welded steel joints against static loading. *Engineering Fracture Mechanics*, 136, pp. 38-57, 2015.

combined together through empirical formulas which are derived either from the maximum principal stress criterion or from von Mises equivalent stress [11].

Although effort is being made to develop new optimised technological solutions [6], examination of the state of the art [13] suggests that available methods for designing welded joints against static loading are still based on the use of conventional nominal quantities, the reference document being the report published by the International Institute of Welding (IIW) back in 1968 [14]. The main limitations in efficiently using nominal quantities to address problems of practical interest can be summarised as follows: by nature, nominal stresses cannot directly be linked to the intrinsic quality of the manufactured weldments; in the presence of complex geometries, nominal stresses are poorly related to the actual stresses present in the critical areas of the weld that determine the overall static strength of the welded connections being assessed [15]. Further, whilst the aforementioned nominal stress based approaches can be used to perform a conventional static assessment using classic solid mechanics concepts, unfortunately they are not suitable for being used to directly perform an efficient computer aided design (for instance, through the FE method). Lastly, the use of nominal dimensions to calculate the stress quantities of interest prevents the use of stress/strength analyses to optimise the welding variables by simultaneously taking into account the actual morphology of the material microstructure in the vicinity of the assumed crack initiation points.

In this complex scenario, the aim of the present paper is to formalise and validate a novel methodology suitable for designing arc welded joints against static loading by directly post-processing the linear-elastic stress fields damaging the material in the vicinity of the critical locations.

FUNDAMENTALS OF THE THEORY OF CRITICAL DISTANCES

The Theory of Critical Distances (TCD) [16] takes as its starting point the assumption that the static strength of notched/cracked engineering materials can directly be estimated by post-processing the entire linear-elastic stress field acting on the material in the vicinity of the geometrical features being assessed. According to this idea, by changing the shape and size of the adopted integration

Please, cite this paper as: Ameri, A. A. H., Davison, J. B., Susmel, L. On the use of linear-elastic local stresses to design load-carrying fillet-welded steel joints against static loading. *Engineering Fracture Mechanics*, 136, pp. 38-57, 2015.

domain, the TCD effective stress, σ_{eff} , can be calculated in different ways, e.g. the Volume, Area, Line, and Point Method [16, 17].

In order to mathematically formalise the TCD, the initial assumption can be made that the necessary critical distance value, L , is known *a priori*; the strategy to determine it is explained as follows. Consider now the notched component sketched in Figure 1a. This component is assumed to be subjected to a complex system of external forces and moments. Given the boundary conditions, the corresponding linear elastic-stress field can be estimated in the vicinity of the assessed notch tip by solving, for instance, a conventional linear-elastic FE model.

The most complex formalisation of the TCD, which is known as the Volume Method (VM) [17], postulates that the effective stress, σ_{eff} , has to be derived by averaging the chosen equivalent stress (i.e., Von Mises, Tresca, maximum principal stress criterion, etc. [18-21]) over an hemisphere centred at the apex of the stress raiser. If the problem is simplified by considering a bi-dimensional integration domain, the effective stress, σ_{eff} , can be estimated also by averaging the adopted equivalent stress over a semi-circular area centred at the notch tip and having radius equal to critical distance L [21, 22]. This is known as the Area Method (AM) and, according to Figs 1a and 1b, it can be formalised as follows [16]:

$$\sigma_{\text{eff}} = \frac{4}{\pi L^2} \int_0^{\pi/2} \int_0^L \sigma_{\text{eq}}(\theta, r) \cdot r \cdot dr \cdot d\theta \quad (1)$$

In definition (1) linear-elastic equivalent stress σ_{eq} is determined according to one of the classic hypotheses (such as von Mises, Tresca, maximum principal stress criterion, etc.), whereas L is the critical distance value.

The way the effective stress is calculated using either the VM or AM makes it evident that the TCD estimates the static strength of notched/cracked materials by assessing the entire stress field in a specific reference or process zone [16]. In other words, such a process zone can be assumed to represent that portion of material controlling the overall static strength of the component being

Please, cite this paper as: Ameri, A. A. H., Davison, J. B., Susmel, L. On the use of linear-elastic local stresses to design load-carrying fillet-welded steel joints against static loading. *Engineering Fracture Mechanics*, 136, pp. 38-57, 2015.

assessed. In this setting, the size of the process zone is seen to be affected by three primary factors [16, 20], that is, (i) material microstructural features, (ii) local micro-mechanical properties, and (iii) characteristics of the physical mechanisms resulting in the cracking process. According to both the VM and the AM (Fig. 1b), the hypothesis can then be formed that the radius of the volume/area defining the process zone itself approaches critical distance L .

Although both the VM and the AM are very appealing from a philosophical point of view, their in-field usage is not at all straightforward, since *ad hoc* numerical/analytical procedures are needed to accurately average the adopted equivalent stress over the appropriate integration domain. However, by using a sophisticated reasoning based on the Linear-Elastic Fracture Mechanics concepts [22], it is possible to show that the effective stress can also be calculated by considering the stress state at a distance from the notch tip equal to $L/2$. In more detail, according to Figure 1c, σ_{eff} can be derived as follows:

$$\sigma_{\text{eff}} = \sigma_{\text{eq}} \left(\theta = 0^\circ, r = \frac{L}{2} \right) \quad (2)$$

where, again, σ_{eq} is the equivalent stress calculated according to the chosen hypothesis. This formalisation of the TCD is known as the Point Method (PM) [16, 22].

The equivalence between the VM, AM, and PM suggests that the stress state calculated at the centre of the process zone supplies all the engineering information needed to accurately quantify the extent of damage associated with the entire process zone. This obviously results in a great simplification of the design process, since static strength can directly be estimated by simply using the adopted equivalent stress determined at a given material point.

As soon as σ_{eff} is known, the second information which is needed to perform the static assessment is the so-called inherent material strength, σ_0 [16]. Accurate experimental investigations have proven that the actual value of strength σ_0 mainly depends on the mechanical/cracking behaviour displayed by the material being assessed. In more detail, when the processes resulting in the final

Please, cite this paper as: Ameri, A. A. H., Davison, J. B., Susmel, L. On the use of linear-elastic local stresses to design load-carrying fillet-welded steel joints against static loading. *Engineering Fracture Mechanics*, 136, pp. 38-57, 2015.

breakage involve large-scale plastic deformations, σ_0 is seen to take on a value which is larger than the material ultimate tensile strength, σ_{UTS} . In particular the relationship between σ_0 and σ_{UTS} can be written as follows:

$$\sigma_0 = \kappa \cdot \sigma_{UTS} \quad (3)$$

where κ is a material constant larger than unity [16]. This specific behaviour is observed not only in conventional ductile materials such as metals [16, 20, 21], but also in quasi-brittle polymers such as polymethylmethacrylate [18, 23]. On the contrary, inherent material strength σ_0 is seen to be equal to σ_{UTS} - i.e., $\kappa=1$ in Eq. (3) - in those situations in which the effect on the final cracking behaviour of the material non-linearities is absent (as it happens, for instance, in engineering ceramics [24]) or, in any case, very limited (as it happens, for instance, in fibre reinforced composites [25]). In this context, it is important to observe that σ_0 is different from σ_{UTS} also when localised stress concentration phenomena due to notches result in different failure mechanisms to those observed in the un-notched material [26].

Since, in general, it is not possible to define the value of the inherent strength *a priori*, the most reliable way to determine σ_0 is by running appropriate experiments. The experimental procedure to be followed for an accurate determination of σ_0 is described below.

As soon as both effective stress σ_{eff} and inherent strength σ_0 are known, the notched component being assessed is supposed to withstand the applied loading as long as the following condition is assured:

$$\sigma_{eff} \leq \sigma_0, \quad (4)$$

the corresponding local safety factor taking on the following value:

Please, cite this paper as: Ameri, A. A. H., Davison, J. B., Susmel, L. On the use of linear-elastic local stresses to design load-carrying fillet-welded steel joints against static loading. *Engineering Fracture Mechanics*, 136, pp. 38-57, 2015.

$$\gamma = \frac{\sigma_0}{\sigma_{\text{eff}}} \geq 1 \quad (5)$$

As mentioned earlier, the effective stress, σ_{eff} , can be calculated by post-processing the relevant stress fields according to one of the classic hypotheses. In particular, when the TCD is used to design brittle material, the use of the maximum principal stress criterion is recommended [18, 24]. When the TCD is employed to design ductile materials instead, the highest level of accuracy is obtained by applying it along with von Mises equivalent stress, this holding true independently from the degree of multiaxiality of the applied loading [20, 21]. As to the design of ductile metals, it is worth pointing out here that accurate results can be obtained without the need for explicitly modelling the elasto-plastic behaviour of the material being assessed. In other words, although, within the process zone, the local mechanical behaviour of metallic materials is highly non-linear, metallic materials can directly be designed against static loading by simply using a linear-elastic constitutive law to determine the required stress fields [21]. This fact can be justified by using an energy argument as reported by Lazzarin and Zambardi [27] who have proven that the linear-elastic energy equals the elasto-plastic one, when these quantities are averaged within the entire fatigue process zone. From a practical point of view, the fact that a simple linear-elastic constitutive law can be used to determine the relevant stress fields results in a great simplification of the static assessment process, this leading to a reduction of the time and costs associated with the design process.

The reasoning summarised above was based on the assumption that both the critical distance, L , and the material inherent strength, σ_0 , are known *a priori*. According to in-field experience, for a given the material, the most accurate way to determine these two properties is by experimentally determining the static strength of samples containing, at least, two different geometrical features. Figure 1d schematically depicts this experimental strategy, where the two stress-distance curves plotted, in the incipient failure condition, in terms of the adopted equivalent stress obtained by testing a sharp and blunt notch, respectively. According to the PM, the coordinates of the point at which these two curves intersect each other directly gives the values of both L and σ_0 (Fig. 1d).

Please, cite this paper as: Ameri, A. A. H., Davison, J. B., Susmel, L. On the use of linear-elastic local stresses to design load-carrying fillet-welded steel joints against static loading. *Engineering Fracture Mechanics*, 136, pp. 38-57, 2015.

It is worth observing here also that, when the TCD is applied in conjunction with the maximum principal stress criterion, the critical distance value L can be estimated not only according to the procedure sketched in Figure 1d, but also via the following definition [16]:

$$L = \frac{1}{\pi} \left(\frac{K_{Ic}}{\sigma_0} \right)^2, \quad (6)$$

where K_{Ic} is the plane strain fracture toughness.

Having reviewed the fundamentals of the TCD, the aim of this paper is to reformulate this powerful design theory to make it suitable for directly designing steel arc welded joints against static loading.

QUANTITATIVE FORMALISATION OF THE PROPOSED DESIGN METHOD

In order to correctly use the TCD to design welded joints against static loading, the first step is choosing the most appropriate equivalent stress to be used to model the mechanical/cracking behaviour displayed by the material being assessed. Recent testing of notched cylindrical bars of Al6082 under combined tension and torsion has proven [20, 21] that the highest level of accuracy in estimating static strength of notched ductile materials is obtained by applying the TCD along with von Mises equivalent stress. Similar to notched aluminium alloys, steel welded joints experience large-scale localised plastic deformations before breakage takes place. Thus, the hypothesis can be formed that ductile steel arc welded connections can be successfully assessed by employing the PM in conjunction with von Mises equivalent stress, σ_{VM} . It is important to point out here also that, due to the complex profiles of the geometrical features weakening welded joints' critical areas, the corresponding linear-elastic local stress fields are not only characterised by severe gradients (i.e., stress concentration phenomena), but they are also multiaxial. With regard to the latter aspect, it can be noted that the local stress fields are multiaxial even when the external loading applied to the joint being assessed is uniaxial. The considerations briefly reported above seem to strongly support the idea that σ_{VM} is the most appropriate equivalent stress to be used

Please, cite this paper as: Ameri, A. A. H., Davison, J. B., Susmel, L. On the use of linear-elastic local stresses to design load-carrying fillet-welded steel joints against static loading. *Engineering Fracture Mechanics*, 136, pp. 38-57, 2015.

together with the PM to design steel welded connections. In fact, σ_{VM} is capable not only of efficiently modelling the mechanical behaviour of ductile metals, but also of accurately taking into account the degree of multiaxiality of the assessed critical stress state.

After choosing an appropriate equivalent stress, the subsequent step in the reasoning is defining a reference value both for critical distance L and for inherent material strength σ_0 . This will be done by using as reference geometry lap joint with transverse fillet welds.

Consider then the lap joint sketched in Figure 2a. Assume that such a joint is loaded in tension, where F is the applied axial force. As far as fillet welded joints with incomplete penetration are concerned, cracks are observed to initiate at the tip of the weld roots (point O in Figures 2a and 2b). The subsequent propagation is seen to occur, in the filler material, along a direction having angle θ ranging between 0° and 90° (see the values of fracture angle θ_f listed in Table 2) [28], θ being defined as shown in Figure 2c. In steel welded joints the actual orientation of the crack paths mainly depends on the local distribution of the stress as well as on the metallurgical microstructural features of the weld metal. In terms of *modus operandi*, as far as stress concentrators are concerned, the TCD works by predicting the initiation (or non-initiation) of cracks [16]. According to the fact that, by nature, the TCD is a crack initiation method, the AM process zone can then be defined as shown in Figure 2d. In particular, the diameter defining the integration semi-circular domain is assumed to be perpendicular to the crack-like notch bisector, the centre of such an area being coincident with the weld tip root. As soon as the equivalent stress averaged over the process zone, Eq. (1), reaches a value equal to the inherent material strength, a crack initiates at the weld root, eventually leading to the complete failure of the welded joint. Since the cracks resulting in the final breakage are seen to propagate mainly in the weld material, the above considerations suggest that the static assessment of load-carrying fillet-welded steel joints can directly be performed according to the TCD by using as reference strength the UTS of the filler material.

As depicted in Figure 2d, the process zone defined according to the AM allows the position of the PM critical point to be defined unambiguously. The PM effective stress is calculated via the stress

Please, cite this paper as: Ameri, A. A. H., Davison, J. B., Susmel, L. On the use of linear-elastic local stresses to design load-carrying fillet-welded steel joints against static loading. *Engineering Fracture Mechanics*, 136, pp. 38-57, 2015.

state acting on a point positioned, along the x axis, at a distance from the root tip equal to $L/2$ (see Figure 2d). In other words, the material point to be used to apply the TCD in the form of the PM is assumed to belong to the crack-like notch bisector, this holding true independently from the complexity of the local stress field damaging the weld seam being assessed. As to the validity of the above assumption, it is worth noticing here that a similar strategy was seen to be successful also in estimating fatigue damage in welded joints having complex geometry [29-31].

Turning back to the estimation of a reference value for both L and σ_o , as briefly mentioned in the previous section, the most accurate way to determine such material properties is by post-processing experimental results generated by testing notches of different sharpness (see Figure 1d). Unfortunately, unless a rounded gap is intentionally introduced, the root radius of the crack-like notch at the weld root is always very small, approaching zero in the majority of the cases [28]. Therefore, if the stress analysis is performed by taking the root radius invariably equal to zero, the resulting local linear-elastic stress fields are not only singular, but also self-similar. This implies that the experimental strategy sketched in Figure 1d is not suitable for directly estimating L and σ_o , since, due to the self-similarity characterising the stress fields, it would be impossible for the position of the intersection point to be located accurately. A different stratagem is then needed to estimate the material properties of interest. The proposed method to determine L and σ_o is explained below.

The chart of Figure 3a summarises the linear-elastic stress distance curves plotted, in the incipient failure condition, along the crack-like notch bisector (i.e., for $\theta=0^\circ$) in terms of von Mises equivalent stress. In this chart, σ_{VM} is normalised with respect to the ultimate tensile strength, σ_{UTS} , of the filler material. The experimental results used to plot the above normalised stress fields are listed in Table 2, the dimensions of the investigated welded joints being defined as shown in Figure 2a. The mechanical properties of both the parent and the filler material are reported in Table 1.

The required stress fields were determined by solving simple bi-dimensional linear-elastic Finite Element (FE) models using commercial software ANSYS®. The investigated lap joints were modelled by using bi-dimensional elements Plane 183, i.e., a higher order 8-node element with

Please, cite this paper as: Ameri, A. A. H., Davison, J. B., Susmel, L. On the use of linear-elastic local stresses to design load-carrying fillet-welded steel joints against static loading. *Engineering Fracture Mechanics*, 136, pp. 38-57, 2015.

quadratic displacement behaviour where each node has two degrees of freedom. The linear-elastic stress-distance curves plotted in Figure 3 were determined by increasing the mesh density in the vicinity of the weld roots. In particular, bearing in mind that these stress fields were singular, the mesh size was gradually reduced until profile and magnitude of the local linear-elastic stress-distance curves were no longer affected by the mesh density itself in a region characterised by r larger than 0.5 mm. This resulted in elements in the vicinity of the weld root having size equal to about 0.07 mm. It is also important to observe that the above stress fields were calculated under a plane strain hypothesis. This assumption derives from the fact that, in joints with transverse fillet welds, cracks are seen to initiate mainly at the mid-section of the joints themselves, i.e., at that section experiencing the largest degree of triaxiality of the local stress fields. Owing to the fact that the width of the investigated lap joints was large compared to the weld dimensions, the simplifying hypothesis was formed that the critical sections were subjected to plane strain.

Turning back to the chart of Figure 3a, according to the PM, the critical stress has to be calculated at a distance from the assumed crack initiation location equal to $L/2$ – see Eq. (2). Five different lengths were considered to estimate a reliable reference value for quantity $L/2$, i.e., $r=2, 2.5, 3, 3.5, 4$ mm. For any of these lengths, the linear-elastic stress-distance curves determined in the incipient failure condition allowed the mean value of the σ_{VM} to σ_{UTS} ratio and its standard deviation, S_D , to be calculated directly. According to the values reported in the above diagram, both the mean value and the standard deviation tend to decrease as r increases, S_D reaching its minimum value at a distance from the crack-like notch tip equal to 3.5 mm. This suggests that the minimum level of dispersion is obtained for $r \geq 3.5$ mm. According to the PM's *modus operandi*, given the profile and magnitude of the stress-distance curve, the effective stress calculated via Eq. (2) increases as $L/2$ decreases. This implies that, for a given value of inherent strength σ_o , the level of conservatism in estimating static strength increases as σ_{eff} calculated through definition (2) increases. This reasoning suggests that the critical distance value, L , for steel arc welded joints can be taken equal to 7 mm, since $r=3.5$ mm is the shortest distance at which the standard deviation reaches its

Please, cite this paper as: Ameri, A. A. H., Davison, J. B., Susmel, L. On the use of linear-elastic local stresses to design load-carrying fillet-welded steel joints against static loading. *Engineering Fracture Mechanics*, 136, pp. 38-57, 2015.

minimum value. Thus, the distance to apply the PM to design steel arc welded joints against static loading can be taken as follows:

$$\frac{L}{2} = 3.5 \text{ mm} \quad (7)$$

It is worth noticing that when the TCD is used to design welded joints against fatigue [29-31], the recommended values for critical distance L are, at least, an order of magnitude lower than the value proposed here to be used to perform the static assessment. This fact is not surprising as very often the L values under static loading for structural metallic materials are seen to be of the order of several millimetres [16]. For instance, the experimental value of the static critical distance for commercial cold-rolled low-carbon steel En3B is equal to 7.4 mm [19], this length being very close to the one suggested above as being employed to design steel welded joints against static loading. The large values of length L characterising ductile metals can simply be ascribed to the fact that, in these materials, final breakage under static loading is preceded by large scale plastic deformations resulting in extended process zones [16, 19]. In contrast, in welded joint failing in the medium/high-cycle fatigue regime, the cyclic plastic regions in the vicinity of the crack initiation locations are quite small [29-31], this resulting in turn in small values for the corresponding critical distance.

The mean values of the σ_{VM} to σ_{UTS} ratio represent instead the central tendency of constant κ in Eq. (3) as the distance, r , from the weld root increases. As shown in the chart of Figure 3a, κ is equal to 1.39 for $r=3.5$ mm, whereas it is equal to 1.37 for $r=4$ mm. Therefore, to guarantee an adequate level of safety, the inherent strength is suggested here as being estimated by taking $\kappa=1.35$ in Eq. (3), i.e.:

$$\sigma_0 = 1.35 \cdot \sigma_{UTS} \quad (8)$$

Please, cite this paper as: Ameri, A. A. H., Davison, J. B., Susmel, L. On the use of linear-elastic local stresses to design load-carrying fillet-welded steel joints against static loading. *Engineering Fracture Mechanics*, 136, pp. 38-57, 2015.

where σ_{UTS} is the ultimate tensile strength of the filler material.

As briefly discussed above, since the TCD is a crack initiation approach, the process zone was defined with respect to the crack-like notch bisector (i.e. $\theta=0^\circ$ in Figure 2c). In order to further check the validity of such an assumption, the charts of Figures 3b, 3c, and 3d show the normalised stress-distance curves for θ equal to 15° , 30° and 45° , respectively. These diagrams clearly show that, independently from the considered distance from the weld root tip, the standard deviation is larger than the corresponding one calculated for $\theta=0^\circ$. This should further confirm that the highest level of accuracy in using the PM to design lap joints with transverse fillet welds is obtained by employing the $\theta=0^\circ$ direction to define the process zone (see Figure 2d).

In order to quantify the accuracy of the PM applied by taking $L/2=3.5$ mm and $\sigma_o=1.35\cdot\sigma_{UTS}$, Table 2 lists, for any considered experimental results, the error made in estimating the static strength of the considered welded joints, the error being calculated as:

$$\text{Error} = \frac{\sigma_{\text{eff}} - \sigma_0}{\sigma_0} [\%] \quad (9)$$

According to the above definition, an error larger than zero indicates a conservative estimate, whereas a negative error denotes a non-conservative prediction. Table 2 shows that the use of the PM with $L/2=3.5$ mm and $\sigma_o=1.35\cdot\sigma_{UTS}$ resulted in estimates falling mainly within an error interval of $\pm 20\%$.

In order to judge the obtained degree of accuracy, it is worth observing here that, as far as notched un-welded materials are concerned, in general, it is not possible to distinguish between an error of $\pm 20\%$ and an error of 0% due to those problems which are usually encountered during testing as well as during the numerical analyses [16]. In this context, it should be noted that the level of scatter characterising the mechanical and cracking behaviour of engineering materials mainly depends on the specific local microstructural features of the material being assessed. As far as welded joints are concerned, the design problem is further complicated by the fact that their overall

Please, cite this paper as: Ameri, A. A. H., Davison, J. B., Susmel, L. On the use of linear-elastic local stresses to design load-carrying fillet-welded steel joints against static loading. *Engineering Fracture Mechanics*, 136, pp. 38-57, 2015.

strength depends not only on the microstructural characteristics of the employed metals, but also on the way the technological variables are set to manufacture the welds. This clearly suggests that using a target error interval of $\pm 20\%$ should allow a severe verdict about the overall accuracy of the proposed method to be expressed.

Even if the obtained level of accuracy is certainly encouraging, it is evident that this was obtained by considering the same data as those employed to calibrate the method itself. This implies that a more rigorous and comprehensive validation exercise must be performed in order to be able to judge whether the proposed approach can safely be used in situations of practical interest to design steel arc welded joints against static loading. This will be done in the next section by considering three-dimensional welded geometries.

Before moving to welded connections having complex geometry, it is worth observing here that, according to the PM's philosophy, the critical point must be taken at a distance from the assumed crack initiation point equal to $L/2$. For the sake of consistency, such a critical point must always be positioned at a distance at least equal to $L/2$ from any other free surfaces. As it will be discussed in the next section, this important rule must always be borne in mind in order to accurately perform the static assessment of three-dimensional welded connections according to the proposed approach.

In brief, the fundamental assumptions made to re-formulate the TCD to make it suitable for designing steel arc welded joints against static loading can be summarised as follows:

- the mechanical behaviour of both the parent and the filler material is modelled by adopting a linear-elastic constitutive law;
- the linear-elastic multiaxial local stress fields have to be recalculated in terms of von Mises equivalent stress;
- unless the value of the root radius is known, weld roots are modelled as sharp crack-like notches;
- the critical distance value, L , is taken as 7 mm (i.e., $L/2=3.5$ mm);

Please, cite this paper as: Ameri, A. A. H., Davison, J. B., Susmel, L. On the use of linear-elastic local stresses to design load-carrying fillet-welded steel joints against static loading. *Engineering Fracture Mechanics*, 136, pp. 38-57, 2015.

- the inherent material strength, σ_o , is taken equal to $1.35 \cdot \sigma_{UTS}$, where σ_{UTS} is the ultimate tensile strength of the filler material;
- the PM is applied by considering those material points belonging to the plane containing the crack-like notch bisectors;
- the material point used to apply the TCD in the form of the PM must be at a distance from any free surfaces larger than (or, at least, equal to) $L/2=3.5$ mm.

To conclude it is worth observing that, according to the above limitations, the proposed approach cannot be used to design weld seams having length lower than 7 mm. Further, considering that as the thickness of the welded joint being assessed decreases the role played by plasticity becomes more and more relevant, it is not advisable to use the proposed approach to perform the static assessment of welded joints having weld leg length and main plate thickness lower than 5 mm.

VALIDATION BY EXPERIMENTAL DATA

In order to investigate the accuracy of the proposed reformulation of the TCD in estimating the static strength of steel arc welded joints experiencing complex local states of stress in the vicinity of the weld roots, a large number of suitable experimental results were taken from the technical literature.

Independently from the complexity of the investigated welded geometry, the relevant stress fields were determined via commercial software ANSYS® by solving three-dimensional FE models. To reduce the computational time required to obtain the necessary information, the stress analyses were performed by following a conventional solid-to-solid sub-modelling procedure. The investigated three-dimensional geometries were meshed by using ten-node tetrahedral elements Solid 187. This element is characterised by a quadratic displacement behaviour and is defined by ten nodes with three degrees of freedom each. It is worth observing here that the investigated samples were all modelled by using the actual dimensions not only of the parent material plates, but also of the weld seams.

Please, cite this paper as: Ameri, A. A. H., Davison, J. B., Susmel, L. On the use of linear-elastic local stresses to design load-carrying fillet-welded steel joints against static loading. *Engineering Fracture Mechanics*, 136, pp. 38-57, 2015.

Considering that the PM reference length was known *a priori* (i.e., $L/2=3.5$ mm), the convergence analyses were done by targeting the stress distribution at a distance from the weld root larger than 2 mm. Since the area of interest was relatively far away from the singularity regions, elements having a size of 0.125 mm were seen to be small enough to accurately determine the required stress fields, this holding true independently from the complexity of the investigated welded joint's geometry.

Initially, the accuracy of the PM in estimating static strength of welded connections was checked by considering longitudinal fillet weld specimens subjected to axial loading. The geometry of these samples is shown in Figure 4a. The re-analysed experimental results are summarised in Table 3, whereas the mechanical properties of both the parent and the filler material are reported in Table 1. By considering specimen 1-2-L-0 [9] (see Table 3), the chart reported in Figure 4 exemplifies how the stress analysis was performed in order to calculate the effective stress according to the PM for this specific welded geometry. In particular, linear coordinate r was taken parallel to the longitudinal weld root straight line, the origin being positioned at the edge of the weld seam at a distance from the weld root tip equal to $L/2=3.5$ mm (see Figure 4a). According to the assumption made to define the process zone in welded joints (see Figure 2d), coordinate r lies on that plane containing, at any section of the weld, the crack-like notch bisector (i.e., a plane coincident with the surface of the main plate). The chart of Figure 4b shows, in the incipient failure condition, the distribution of von Mises equivalent stress, σ_{VM} , along linear coordinate r . It is interesting to observe that, according to the specific geometrical features of the investigated welded joint, given the weld seam, there are two regions where the local stresses diverge to infinity, i.e., the weld root line and the corner resulting from the intersection between the weld bead and the main plate (i.e., as shown in Figure 4b, the corner edge to which origin O belongs). Since according to the PM's *modus operandi* the material point used to calculate the effective stress must be at a distance from any free surfaces larger than $L/2$, the stress states damaging, over a length of 3.5 mm, both the weld start and the weld end regions were not considered. As shown in Figure 4b for the specific case of specimen 1-2-L-0 [9] (see Table 3), for all the investigated longitudinal fillet weld samples,

Please, cite this paper as: Ameri, A. A. H., Davison, J. B., Susmel, L. On the use of linear-elastic local stresses to design load-carrying fillet-welded steel joints against static loading. *Engineering Fracture Mechanics*, 136, pp. 38-57, 2015.

the critical point (i.e., the material point experiencing the largest von Mises equivalent stress) was seen to be at a distance r from the weld start equal to 3.5 mm. The error values listed in Table 3 and calculated according to definition (9) prove that the proposed design method was capable of accurately estimating the static strength of such welded joints, resulting in predictions mainly falling within an error interval of $\pm 20\%$. Such a level of accuracy is certainly remarkable, especially in light of the fact that, compared to the reference geometrical configuration used in the previous section to estimate both L and σ_o , in these specimens the weld seams were parallel (and not perpendicular) to the direction along which the axial loading was applied. This suggests also that the proposed approach may be used to estimate the static strength of lap joints subjected to prevalent mode II loading.

Subsequently, the proposed TCD based approach was attempted to be used to estimate the static strength of uniaxially loaded specimens with combined longitudinal and transverse fillet welds, the geometry of these specimens being sketched in Figure 5b. Table 4 summarises the considered experimental results, whilst the mechanical properties of both the parent and the filler material are listed in Table 1.

To exemplify how this welded geometry was post-processed, the charts of Figure 5b and 5c report, for specimen TL50-1 [34] (see Table 4), the von Mises stress distribution in the incipient failure condition along the transverse and longitudinal fillet weld, respectively. For the two weld seams, linear coordinates r were defined as shown in Figure 5a, such linear coordinates again lying on those planes containing, at any section of the weld seams, the crack-like notch bisector. Similar to what was done above, the stress states damaging over a length of 3.5 mm both the weld start and the weld end regions were disregarded. According to the stress analysis shown in the charts of Figure 5 for the specific case of specimen TL50-1 [34], for this welded geometry the critical point (i.e., the point within the region of interest experiencing the maximum value of the von Mises equivalent stress) was seen to be always at a distance equal to 3.5 mm from the end of the longitudinal fillet weld (see Figure 5c). According to the error values reported in Table 4, the PM proved to be highly accurate in predicting the static strength of specimens with combined

Please, cite this paper as: Ameri, A. A. H., Davison, J. B., Susmel, L. On the use of linear-elastic local stresses to design load-carrying fillet-welded steel joints against static loading. *Engineering Fracture Mechanics*, 136, pp. 38-57, 2015.

longitudinal and transverse fillet welds, resulting in estimates falling within an error interval of $\pm 15\%$.

To further check the accuracy and reliability of the proposed design approach, the PM was subsequently attempted to be used also to estimate the static strength of the specimens with inclined welds sketched in Figure 6a. The considered experimental results are listed in Table 5, whereas the mechanical properties of the parent and filler material are reported in Table 1.

In order to re-analyse this welded geometry, the reference linear coordinate, r , was defined as shown in Figure 6a. In particular, such a coordinate was taken parallel to the weld root line, the origin being positioned at a distance from the weld root itself equal to 3.5mm. Again, coordinate r lies on that plane containing, at any section of the weld, the crack-like notch bisector.

As shown in Figure 6b for the specific case of specimen F1-1 [33], the critical point in the investigated inclined fillet weld specimens was seen to be always at a distance from the weld start equal to 3.5 mm.

The error values listed in Table 5 show that the proposed design method was highly accurate for series E1, but slightly too conservative for series E2 and E3. According to what is reported in the original source [33], this could simply be ascribed to the very high quality characterising the welds of series E2 and E3.

The last geometry which was considered to check the accuracy of the proposed TCD based approach is shown in Figure 7a. Gomez et al. [35] investigated the static strength of cruciform welded joints loaded in out-of-plane three-point bending, the testing set-up being schematically shown in Figure 7a. The experimental results for this specific geometry/loading configuration are reported in Table 6. The mechanical properties of both the parent and the filler material are summarised in Table 1.

In order to determine the relevant linear-elastic stress distributions, linear coordinate r was defined as shown in Figure 7a and was taken parallel to the weld root straight line with its origin O being at the weld start. As before, this linear coordinate lies on the plane containing, at any section of the weld, the crack-like notch bisector.

Please, cite this paper as: Ameri, A. A. H., Davison, J. B., Susmel, L. On the use of linear-elastic local stresses to design load-carrying fillet-welded steel joints against static loading. *Engineering Fracture Mechanics*, 136, pp. 38-57, 2015.

The chart of Figure 7b shows, in the incipient failure condition, the stress distribution along coordinate r for sample B_125_A516_55_1 [35] (see also Table 6). Since the stress field was post-processed according to von Mises' hypothesis, the local equivalent stress is positive not only on the tension, but also on the compression side. The stress states damaging over a length of 3.5 mm both the weld start and the weld end regions were disregarded since, as postulated by the PM, the material point to be used to calculate the effective stress must be at a distance from any free surfaces larger than $L/2$. Considering that, as expected, in these samples cracks initiated on the specimen side subjected to tensile stress, the critical point was seen to be always positioned, along coordinate r , at a distance from the weld end equal to 3.5 mm (see Figure 7b).

The error values reported in Table 6 confirm that the PM was highly accurate in estimating the static strength of this specific geometry/loading configuration, resulting in predictions falling mainly within an error interval of $\pm 15\%$.

To conclude, the overall accuracy of the proposed PM based design method is summarised in the semi-logarithmic diagram reported in Figure 8a. This chart was built by plotting the error against the ratio between the weld leg, s , and the main plate reference thickness, T , such a ratio being representative of the scale effect. This chart makes it evident that our approach is highly accurate, resulting in estimates mainly failing within an error interval of $\pm 20\%$. Such a remarkable level of accuracy is obtained independently from geometry/loading configuration, absolute dimensions of both the joint and the weld, mechanical properties of the parent and filler material, and adopted welding technology. Such a high level of accuracy (Fig. 8a) strongly supports the idea that the proposed PM based approach is a powerful engineering tool suitable for accurately performing the static assessment of welded joints in situations of practical interest.

DISCUSSION

By taking as a starting point the fundamental concepts on which the Theory of Critical Distances is based, the present paper summarises a novel linear-elastic local stress based approach suitable for designing steel arc welded joints against static loading.

Please, cite this paper as: Ameri, A. A. H., Davison, J. B., Susmel, L. On the use of linear-elastic local stresses to design load-carrying fillet-welded steel joints against static loading. *Engineering Fracture Mechanics*, 136, pp. 38-57, 2015.

Examination of the state of the art suggests that the standard methodologies commonly employed in the industrial arena are still based on the use of nominal stresses calculated with reference to a nominal weld throat area. In contrast, the approach proposed in the present paper can be used to perform the static assessment of steel welded joints by directly post-processing the linear-elastic local stress fields acting on the material in the vicinity of the welds being designed. This implies that the overall static strength of welded joints can be assessed by considering the actual criticality of the local stress at any section of the weld seams under investigation.

Owing to the fact that the required stress analysis can be done by assuming that both the parent and the filler material obey a linear-elastic constitutive law, the proposed reformulation of the TCD can be applied by taking full advantage of the results obtained by solving conventional bi- and three-dimensional FE models. In these models the critical areas are assessed by considering the actual geometry and dimensions of the weld seams. This allows the position, within the region of interest, of the critical point to be located unambiguously. As to this aspect, when post-processing the linear-elastic stress fields calculated by solving complex three-dimensional FE models, according to the TCD's *modus operandi*, the assumption was made that the material point to be used to determine the PM effective stress had to be at a distance from any free surfaces larger than (or, at least, equal to) $L/2=3.5$ mm. This resulted in the fact that those regions close to both the weld starts and the weld ends were not considered when locating the position of the critical point itself. As to this aspect, it is interesting to observe that, when the design problem is addressed according to the standard methods [15], under particular circumstances, the actual length of the weld seam is not used to determine the corresponding nominal stresses. This is done either to take into account the non-uniform distribution of the local stresses in weld beads which are "too long" to be safely designed by using nominal stress based approaches, or to consider the presence of welding defects which tend to accumulate themselves at the periphery of the weld seams.

To reanalyse all the experimental data considered in this investigation, the weld roots were treated as crack-like notches, i.e., the tip radius was set invariably equal to zero. This was done because in the majority of the situations the root radius is so small to approach zero. Such an assumption results, of course, in a slightly larger level of conservatism. However, given the material, the TCD's

Please, cite this paper as: Ameri, A. A. H., Davison, J. B., Susmel, L. On the use of linear-elastic local stresses to design load-carrying fillet-welded steel joints against static loading. *Engineering Fracture Mechanics*, 136, pp. 38-57, 2015.

mechanical properties of interest (i.e., L and σ_0) do not depend on the sharpness of the assessed notch [16, 18-21]. Accordingly, in the presence of rounded root gaps having finite radius, the relevant linear-elastic stress fields can directly be determined by modelling the finite notch radius explicitly. This would allow a higher degree of accuracy in estimating static strength to be reached.

It is interesting to highlight here also that if the crack-like notch radius is taken equal to zero, the relevant linear elastic stress fields in standard welded joints can directly be estimated by taking full advantage of the Linear Elastic Fracture Mechanics (LEFM) concepts (see, for instance, Ref. [10, 36-39] and references reported therein). As to this *modus operandi*, attention must be paid when the LEFM equations are employed to determine the required stress state at a distance from the weld root equal to $L/2=3.5$ mm. In fact, according to the geometry and absolute dimensions of the joint being designed, the material point of interest may be positioned in a region where the stress distribution depends not only on the geometrical singularity, but also on the nominal stress. Accordingly, under these particular circumstances, it is always advisable to double-check the magnitude of the estimated equivalent stress via conventional linear-elastic FE models.

Another key aspect which is worth being mentioned is that, by its nature, the TCD can be used to efficiently assess the detrimental effect of micro-cracks and flaws [16]. Accordingly, if accurately validated against appropriate experimental results, the PM based approach proposed in the present paper could be employed for weld quality management by explicitly modelling the presence of welding defects.

To apply the TCD to assess the detrimental effect of stress concentrators of all kinds, two specific material properties are needed, i.e., the critical distance L and the inherent strength σ_0 . By following a fairly articulated reasoning, we came to the conclusion that, to effectively design steel arc welded joints against static loading, σ_0 has to be taken equal to $1.35 \cdot \sigma_{UTS}$. The fact that σ_0 is larger than σ_{UTS} can be explained by using two different arguments. Materials contain microstructural defects and flaws, the resulting localised stress concentration phenomena affecting the magnitude of the ultimate tensile strength. In the presence of macroscopic geometrical features, the resulting stress concentration phenomena prevail over the localised distortion of the

Please, cite this paper as: Ameri, A. A. H., Davison, J. B., Susmel, L. On the use of linear-elastic local stresses to design load-carrying fillet-welded steel joints against static loading. *Engineering Fracture Mechanics*, 136, pp. 38-57, 2015.

stress field due to the microstructural flaws. Accordingly, inherent material strength σ_o is larger than σ_{UTS} because it quantifies the defect-free strength of the material being assessed [16]. Alternatively, one may argue that σ_o is larger than σ_{UTS} because the process zone is nothing but a damaged enclave surrounded by an un-damaged elastic matrix. The confinement effect of the material surrounding the process zone intrinsically strengthens the material portion where the damage accumulates itself, leading to an increment of the local reference strength. Even if the above arguments seem to be both capable of offering plausible reasons justifying the fact that σ_o is larger than σ_{UTS} , it is evident that more work needs to be done in order to convincingly explain why, in ductile materials, the local inherent strength to be used together with the TCD is larger than the conventional ultimate tensile strength.

From a design point of view, the fact that $\sigma_o=1.35\cdot\sigma_{UTS}$ has two interesting important implications. In particular, when the PM is applied by taking $L/2=3.5$ mm and $\sigma_o=1.35\cdot\sigma_{UTS}$, since, according to Figure 8a, such an approach results in estimates mainly falling within an error interval of $\pm 20\%$, welded joints are recommended to be designed in situation of practical interest by adopting a local safety factor, Eq. (5), always larger than 1.25. The second important implication is shown by the error diagram reported in Figure 8b. In more detail, if $L/2$ is kept constant and equal to 3.5 mm, one may argue that the inherent strength could directly be taken equal to the ultimate tensile strength of the filler material – i.e., $\kappa=1$ in Eq. (3). According to the chart of Figure 8b, such an assumption obviously results in a larger degree of conservatism, with no estimates being on the non-conservative side. Having pointed out these two important aspects, it is worth emphasizing here that the proposed TCD based design approach should be applied by bearing in mind the important suggestions in terms of both reference strength, effect of the technological variables, and level of safety which are given by the available standard codes [15].

As shown by the error chart of Figure 8a, the proposed method's accuracy obtained by taking $L/2=3.5$ mm and $\sigma_o=1.35\cdot\sigma_{UTS}$ is certainly remarkable. But, is the PM more accurate than the standard approach recommended by Eurocode 3? For the welded geometries considered in the present investigation, Table 7 compares the accuracy of the PM to the accuracy obtained by

Please, cite this paper as: Ameri, A. A. H., Davison, J. B., Susmel, L. On the use of linear-elastic local stresses to design load-carrying fillet-welded steel joints against static loading. *Engineering Fracture Mechanics*, 136, pp. 38-57, 2015.

applying, as suggested by Eurocode 3 [15], both the Directional Method and the Simplified Method.

The error values reported in this table were calculated as follows:

$$\text{Error} = \frac{F_{f,\text{exp}} - F_{f,\text{est}}}{F_{f,\text{est}}} [\%] \quad (10)$$

where $F_{f,\text{exp}}$ and $F_{f,\text{est}}$ are the experimental and estimated value of the failure force, respectively. According to the above definition, a negative value of the error denotes a non-conservative estimate. It is worth observing here that, in order to perform a consistent comparison amongst the three design methods, Eurocode 3's approaches were applied by taking factors β_w and γ_{M2} equal to unity, the two suggested design formulas being considered to apply the Directional Method (please, refer to Eurocode 3 [15] for a detail description of these two standard methods as well as for the definition of factors β_w and γ_{M2}). A simple criterion was adopted to select the experimental results used to compile Table 7: for any considered geometry, the first experimental result reported in the original source was considered. According to this table, the use of the PM with $L/2=3.5$ mm and $\sigma_0=1.35\cdot\sigma_{UTS}$ resulted in a larger level of accuracy, the only exception being test 1-2-L-0 (see Table 3) which was generated by Bowman et al. [9] by testing, under axial loading, a longitudinal fillet weld specimen. This can simply be ascribed to the fact that the standard approaches recommended by Eurocode 3 were specifically devised and optimised to perform the static assessment of longitudinal fillet welds. In contrast, the proposed approach was calibrated by using lap joints with transverse fillet welds. However, the error values listed in Table 7 strongly support the idea that the proposed approach can safely be used in situation of practical interest to design steel arc welded joints against static loading and with a higher level of accuracy.

To conclude, it can be highlighted that the obtained accuracy is very promising also because, via σ_0 and L , the TCD could directly be linked not only to the actual microstructural features of the material in the process zone, but also to the technological variables defining the welding process. Further, since this approach allows the size of the weld beads to be optimised section by section, if

Please, cite this paper as: Ameri, A. A. H., Davison, J. B., Susmel, L. On the use of linear-elastic local stresses to design load-carrying fillet-welded steel joints against static loading. *Engineering Fracture Mechanics*, 136, pp. 38-57, 2015.

properly applied and implemented, in the near future such an approach may allow the amount of energy and material used to manufacture welded joints to be reduced. These considerations suggest that such an alternative way of designing welded joints certainly represents an interesting research avenue which deserves to be investigated further.

CONCLUSIONS

- The PM is recommended to be employed to design steel arc welded joints against static loading by taking $L/2=3.5$ mm and $\sigma_0=1.35\cdot\sigma_{UTS}$ (where σ_{UTS} is the tensile strength of the filler material).
- The linear-elastic multiaxial local stress fields needed to determine the PM effective stress are suggested as being recalculated in terms of von Mises equivalent stress;
- Unless the value of the root radius is known, weld roots can directly be modelled as sharp crack-like notches.
- The systematic validation exercise performed to check the accuracy and reliability of the proposed approach proves that this novel design method is capable of estimates falling within an error interval of $\pm 20\%$.
- The proposed approach is recommended to be used in situations of practical interest by adopting a local safety factors larger than 1.25.
- More work needs to be done in this area to rigorously link both L and σ_0 to the microstructural features of the material in the vicinity of the welds as well as to the technological parameters affecting the welding process.

REFERENCES

- [1] Reed RP, Smith JH, Christ BW. The Economic Effects of Fracture in the United States. U.S. Department of Commerce, National Bureau of Standards, Special Publication 647, March 1983.
- [2] Faria L. The economic effect of fracture in Europe. Final report of European Atomic Energy Community study contract no. 320105, 1991.
- [3] Tewari SP, Gupta A, Prakash J. Effect of welding parameters on the weldability of material. *Int J Engng Sci Tech (IJEST)* 2010;2(4):512-516.

Please, cite this paper as: Ameri, A. A. H., Davison, J. B., Susmel, L. On the use of linear-elastic local stresses to design load-carrying fillet-welded steel joints against static loading. *Engineering Fracture Mechanics*, 136, pp. 38-57, 2015.

- [4] Weman K. *Welding processes handbook*. Woodhead Publishing Limited, Cambridge, UK, 2011.
- [5] Davison J B and Owens G W (editors) *The Steel Designers' Manual*, 7th edition, Wiley-Blackwell, 2012
- [6] Mellora BG, Rainey RCT, Kirk NE. The static strength of end and T fillet weld connections. *Mater Design* 1999;20:193-205.
- [7] Mansell DS, Yadav AR. Failure mechanisms in fillet welds. In: *Proc. of Eight Australian Conference on Mechanics of Structures and Materials (ACMSM 8)*, pp. 25.1-25.6, 1982.
- [8] Pham L. Co-ordinated Testing of Fillet Welds Part 1 – Cruciform Specimens. *Australian Welding Research* 1983;12:16-25.
- [9] Bowman MD, Quinn BP. Examination of Fillet Weld Strength. *AISC Engineering Journal* 1994; 31-3:98-108.
- [10] Frank H, Fisher JW. Fatigue strength of fillet welded cruciform joints. *ASCE, Journal of the Structural Division* 1979;20:1727–1740.
- [11] Gillemot LF. Brittle fracture of welded materials. *Proceedings of the 2nd Commonwealth Welding Conference*, London, UK, 1965, pp. 353–358.
- [12] Swannell P. Rational design of fillet weld groups. *ASCE, Journal of the Structural Division Vol.* 1981;107-ST5:789-802.
- [13] Ng AKF, Driver RG, Groding GY. Behaviour of transverse fillet welds. *Structural Engineering Report No. 245*, University of Alberta, Canada, October 2002.
- [14] Ligtenburg FK. *International Test Series, Final Report*. International Institute of Welding, IIW Document XV-242-68, 1968.
- [15] Anon. ENV 1993-1-1, EUROCODE 3 – Design of steel structures, 1988.
- [16] Taylor D. *The Theory of Critical Distances: A new perspective in fracture mechanics*. Elsevier 2007.
- [17] Bellett D, Taylor D, Marco S, Mazzeo E, Guillois J, Pircher T. The fatigue behaviour of three-dimensional stress concentrations. *Int J Fatigue* 2005;27:207-221.
- [18] Susmel L, Taylor D, The theory of critical distances to predict static strength of notched brittle components subjected to mixed-mode loading. *Eng Frac Mech* 2008;75(3-4):534-550.
- [19] Susmel L, Taylor D. On the use of the Theory of Critical Distances to predict static failures in ductile metallic materials containing different geometrical features. *Eng Fract Mech* 2008;75:.4410-4421.
- [20] Susmel L., Taylor D., The Theory of Critical Distances to estimate the static strength of notched samples of Al6082 loaded in combined tension and torsion. Part I: Material cracking behaviour. *Eng Fract Mech* 2010;77:452–469.
- [21] Susmel L, Taylor D. The Theory of Critical Distances to estimate the static strength of notched samples of Al6082 loaded in combined tension and torsion. Part II: Multiaxial static assessment. *Eng Fract Mech* 2010;77:470–478.
- [22] Taylor D. Geometrical effects in fatigue: a unifying theoretical model. *Int J Fatigue* 1999;21:413-420.
- [23] Taylor D, Merlo M, Pegley R, Cavatorta MP. The effect of stress concentrations on the fracture strength of polymethylmethacrylate. *Mater Sci Eng* 2004;A382:288–94.
- [24] Taylor D. Predicting the fracture strength of ceramic materials using the theory of critical distances. *Eng Fract Mech* 2004;71:2407-2416.

Please, cite this paper as: Ameri, A. A. H., Davison, J. B., Susmel, L. On the use of linear-elastic local stresses to design load-carrying fillet-welded steel joints against static loading. *Engineering Fracture Mechanics*, 136, pp. 38-57, 2015.

[25] Whitney JM, Nuismer RJ. Stress Fracture Criteria for Laminated Composites Containing Stress Concentrations. *J Compos Mater* 1974;8:253-65.

[26] Taylor D, Cornetti P, Pugno N. The fracture mechanics of finite crack extension. *Eng Fract Mech* 2005;72:1021-1038.

[27] Lazzarin P, Zambardi R. The equivalent strain energy density approach re-formulated and applied to sharp V-shaped notches under localized and generalized plasticity. *Fatigue Fract Engng Mater Struct* 2002;25:917-928.

[28] Cerit M, Hosgor K, Ayhan AO. Fracture mechanics-based design and reliability assessment of fillet welded cylindrical joints under tension and torsion loading. *Eng Fract Mech* 2014;116: 69-79.

[29] Susmel L. Modified Wöhler Curve Method, Theory of Critical Distances and EUROCODE 3: a novel engineering procedure to predict the lifetime of steel welded joints subjected to both uniaxial and multiaxial fatigue loading. *Int J Fatigue* 2008;30:888-907.

[30] Susmel L. The Modified Wöhler Curve Method calibrated by using standard fatigue curves and applied in conjunction with the Theory of Critical Distances to estimate fatigue lifetime of aluminium weldments. *Int J Fatigue* 2009;31:197-212.

[31] Susmel L. Four stress analysis strategies to use the Modified Wöhler Curve Method to perform the fatigue assessment of weldments subjected to constant and variable amplitude multiaxial fatigue loading. *Int J Fatigue* 2014;64:38-54.

[32] Ng AKF, Driver RG, Gronding GY. Behaviour of transverse fillet welds. *Structural Engineering Report No. 245*, University of Alberta, Department of Civil & Environmental Engineering, 2002.

[33] Deng K, Gronding GY, Driver RG. Effect of loading angle on the behaviour of fillet welds. *Structural Engineering Report No. 251*, University of Alberta, Department of Civil & Environmental Engineering, 2003.

[34] Callele LJ, Grondin GY, Driver RG. Strength and behaviour of multi-orientation fillet weld connections. *Structural Engineering Report No. 255*, University of Alberta, Canada, Department of Civil & Environmental Engineering, 2005.

[35] Gomez I, Kwan YK, Kanvinde A, Grodin G. Strength and ductility of welded joints subjected to out-of-plane bending. Final Report Presented to American Institute of Steel Construction - July 2008 (available at: www.aisc.org)

[36] Niu X, Glinka G. The weld profile effect on stress intensity factors in weldments. *Int J Fracture* 1987;35(1):3-20.

[37] Lukas P. Stress intensity factor for cracks in a fillet welded joint. *Welding International*, 1988;2(5):480-483.

[38] Hobbacher A. Stress intensity factors of plates under tensile load with welded-on flat side gussets. *Eng Fract Mech* 1992;41(6):897-96 1992.

[39] Hobbacher A., Stress intensity factors of welded joints. *Eng Fract Mech* 1993;46(2):173-182.

List of Captions

- Table 1.** Designation and mechanical properties of the investigated parent and filler materials.
- Table 2.** Summary of the experimental results generated by testing lap joints with transverse fillet welds under axial loading (see also Figure 2).
- Table 3.** Summary of the experimental results generated by testing longitudinal fillet welds under axial loading (see also Figure 4a).
- Table 4.** Summary of the experimental results generated by testing combined longitudinal and transverse fillet welds under axial loading (see also Figure 5a).
- Table 5.** Summary of the experimental results generated by testing inclined fillet welds under axial loading (see also Figure 6a).
- Table 6.** Summary of the experimental results generated by testing cruciform welded joints under out-of-plane three-point bending (see also Figure 7a).
- Table 7.** Accuracy of the Point Method, Directional Method [15], and Simplified Method [15] in estimating the static strength of steel arc welded joints.
-
- Figure 1.** Notched component subjected to a complex system of external forces/moments and local system of coordinates (a); effective stress calculated according to the Area (b) and to the Point Method (c); Determination of inherent strength σ_0 and critical distance L via experimental results generated by testing notches of different sharpness (d).
- Figure 2.** Lap joint with transverse fillet welds: technical drawing (a), simplified reference geometry (b), local system of coordinates centred at the tip of the crack-like notch (c), effective stress determined according to the PM (d).
- Figure 3.** Linear-elastic stress distance-curves plotted, in the incipient failure condition, at different values of angle θ for lap joints with transverse fillet welds (see Figure 2 and Table 2).
- Figure 4.** Longitudinal fillet weld specimens (a) and linear elastic stress distribution, in the incipient failure condition, along the weld seam for test 1-2-L-0 [9] (b) – see also Table 3.
- Figure 5.** Combined longitudinal and transverse fillet weld specimens (a); linear elastic stress distribution, in the incipient failure condition, along the transverse (b) and the longitudinal (c) weld seam for test TL50-1 [34] (see Table 4).
- Figure 6.** Inclined fillet weld specimens (a); linear elastic stress distribution, in the incipient failure condition, along the weld seam for test F1-1 [33] (b) – see also Table 5.
- Figure 7.** Cruciform welded joints loaded in out-of-plane three-point bending (a); linear elastic stress distribution, in the incipient failure condition, along the weld seam for test B_125_A516_55_1 [35] (b) - see also Table 6.
- Figure 8.** Overall accuracy of the proposed approach obtained by taking $\sigma_0=1.35\cdot\sigma_{UTS}$ (a) and $\sigma_0=\sigma_{UTS}$ (b).

Tables

Code	Ref.	Parent Material			Filler Material			Welding process ⁽¹⁾		
		Material	σ_y [MPa]	σ_{UTS} [MPa]	E [GPa]	Material	σ_y [MPa]		σ_{UTS} [MPa]	E [GPa]
A	[9]	ASTM A572 gr. 50	345	485	200.0	E7018 Alpha	399	476	209.7	SMAW
B1						E7014 (L-W)	452	520	210.7	
B2						E70T-4 (H-W)	354	535	185.5	
B3						E70-T-4 (L-W)	407	562	203.4	
B4						E70-T-7 (H-W)	468	605	200.8	
B5	[32]	ASTM A572 gr. 50	386	520.5	201.5	E70-T-7 (L-W)	445	584	205.2	FCAW SMAW
B6						E70-T-7 (L-S)	483	652	229.4	
B7						E70T7-K2 (L-W)	527	592	207.1	
B8						E71T18-K6 (H-W)	414	490	199.9	
B9						E71T18-K6 (H-S)	402	493	207.4	
C1						E70T-4	472	631	198.6	
C2	[33]	ASTM A572 gr. 50	366	502	201.5	E70T-7	468	605	200.8	FCAW
C3						E71T8-K6	402	493	207.4	
D1	[34]	ASTM A572 gr. 50	345	485	200.0	ET70-T-7	395	575	193.0	FCAW
D2						ET70-T-7	420	570	195.3	
E1						E70T-4	472	631	198.6	
E2	[33]	ASTM A572 gr. 50	366	502	201.5	E70T-7	468	605	200.8	FCAW
E3						E71T8-K6	402	493	207.4	
F1	[35]	ASTM A572 gr. 50	384	494	200.0	E70T-7	526	670	200.8	FCAW
F2						E70T7-K2	571	672	207.1	

⁽¹⁾SMAW = Shielded Metal Arc Welding; FCAW= Flux Core Arc Welding

Table 1. Designation and mechanical properties of the investigated parent and filler materials.

Code	Ref.	Specimen code	w [mm]	l [mm]	p [mm]	g [mm]	t [mm]	T [mm]	s⁽¹⁾ [mm]	F_f [kN]	θ_r [°]	Error [%]
A	[9]	7-2-T-0	101.6	711.2	254.0	50.8	12.7	25.4	7.9	818	16	-1.2
		8-2-T-0	101.6	711.2	254.0	50.8	12.7	25.4	8.6	845	13	2.7
		9-3-T-0	101.6	711.2	254.0	50.8	19.1	38.1	11.2	1099	14	9.6
		10-4-T-0	101.6	711.2	254.0	50.8	19.1	38.1	11.0	1139	14	11.9
		11-4-T-0	101.6	711.2	254.0	50.8	25.4	50.8	13.4	1303	15	9.7
		12-4-T-0	101.6	711.2	254.0	50.8	25.4	50.8	13.5	1308	16	11.0
B1	[32]	T1-1	76	660	152	3	9.5	19.1	6.3	513	12	-9.9
		T1-2	76	660	152	3	9.5	19.1	6.2	502	8	-11.2
		T1-3	76	660	152	3	9.5	19.1	6.3	513	12	-3.8
		T2-1	76	660	152	3	9.5	19.1	6.1	462	9	-5.4
		T2-2	76	660	152	3	9.5	19.1	6.1	474	14	-10.3
		T2-3	76	660	152	3	9.5	19.1	6.3	482	9	-11.1
		T3-1	76	660	152	3	9.5	19.1	7.4	523	15	-16.7
		T3-2	76	660	152	3	9.5	19.1	7.6	518	18	-21.3
		T3-3	76	660	152	3	9.5	19.1	7.4	520	12	-18.9
		T20-1	76	660	152	3	15.9	25.4	13.7	782	27	-16.0
		T20-2	76	660	152	3	15.9	25.4	13.5	949	7	4.0
		T20-3	76	660	152	3	15.9	25.4	13.7	878	7	-5.9
B2	[32]	T4-1	76	660	152	3	9.5	19.1	6.1	646	0	17.1
		T4-2	76	660	152	3	9.5	19.1	6.2	651	0	15.5
		T4-3	76	660	152	3	9.5	19.1	6.1	629	0	11.8
		T5-1	76	660	152	3	9.5	19.1	6.1	648	0	19.3
		T5-2	76	660	152	3	9.5	19.1	6.2	632	0	14.3
		T5-3	76	660	152	3	9.5	19.1	6.0	628	0	11.2
		T6-1	76	660	152	3	9.5	19.1	5.9	717	90	11.4
		T6-2	76	660	152	3	9.5	19.1	6.0	663	77	17.4
		T6-3	76	660	152	3	9.5	19.1	6.1	741	90	11.4
		T21-1	76	660	152	3	15.9	25.4	12.7	996	0	13.6
		T21-2	76	660	152	3	15.9	25.4	12.9	981	0	16.1
		T21-3	76	660	152	3	15.9	25.4	12.8	921	0	8.0
B3	[32]	T8-2	76	660	152	3	9.5	19.1	6.9	683	6	10.7
		T8-3	76	660	152	3	9.5	19.1	7.1	713	12	13.8
		T23-1	76	660	152	3	15.9	25.4	13.0	966	22	-1.1
		T23-2	76	660	152	3	15.9	25.4	12.9	920	22	-6.3
		T23-3	76	660	152	3	15.9	25.4	13.0	919	17	-6.3

⁽¹⁾Average value of the measured dimensions of the weld leg.

Table 2 (caption on the next page).

Code	Ref.	Specimen code	w [mm]	l [mm]	p [mm]	g [mm]	t [mm]	T [mm]	s ⁽¹⁾ [mm]	F _f [kN]	θ _r [°]	Error [%]
B4	[32]	T11-1	76	660	152	3	9.5	19.1	6.9	695	0	11.0
		T11-2	76	660	152	3	9.5	19.1	7.0	680	0	13.2
		T11-3	76	660	152	3	9.5	19.1	6.9	655	0	-5.4
		T25-2	76	660	152	3	15.9	25.4	12.0	999	0	-8.6
		T25-3	76	660	152	3	15.9	25.4	12.4	1020	11	-11.5
B5	[32]	T13-1	76	660	152	3	9.5	19.1	6.3	607	90	-13.9
		T13-3	76	660	152	3	9.5	19.1	5.8	605	49	-14.5
		T27-1	76	660	152	3	15.9	25.4	12.0	841	25	1.6
		T27-2	76	660	152	3	15.9	25.4	12.0	943	13	-0.5
		T27-3	76	660	152	3	15.9	25.4	11.9	945	13	-6.4
B6	[32]	T14-1	76	660	152	3	9.5	19.1	7.7	769	6	12.4
		T14-2	76	660	152	3	9.5	19.1	7.6	778	8	13.8
		T14-3	76	660	152	3	9.5	19.1	7.5	709	4	9.8
		T15-1	76	660	152	3	9.5	19.1	7.0	781	0	9.1
		T15-2	76	660	152	3	9.5	19.1	7.4	760	0	13.0
		T15-3	76	660	152	3	9.5	19.1	7.2	766	0	10.2
		T28-1	76	660	152	3	15.9	25.4	11.9	990	19	18.6
		T28-2	76	660	152	3	15.9	25.4	11.8	999	0	10.6
T28-3	76	660	152	3	15.9	25.4	12.0	991	0	11.9		
B7	[32]	T16-1	76	660	152	3	9.5	19.1	7.3	769	18	-3.0
		T16-3	76	660	152	3	9.5	19.1	6.9	658	21	4.0
B8	[32]	T18-1	76	660	152	3	9.5	19.1	6.0	711	0	22.0
		T18-2	76	660	152	3	9.5	19.1	5.9	699	0	14.7
		T18-3	76	660	152	3	9.5	19.1	6.1	711	0	14.5
		T31-1	76	660	152	3	15.9	25.4	11.3	1036	0	14.5
		T31-2	76	660	152	3	15.9	25.4	11.5	1004	0	17.3
		T31-3	76	660	152	3	15.9	25.4	11.4	1014	0	24.5
B9	[32]	T19-1	76	660	152	3	9.5	19.1	7.4	780	24	27.1
		T19-2	76	660	152	3	9.5	19.1	7.6	784	26	27.8
		T19-3	76	660	152	3	9.5	19.1	7.5	744	25	22.6
		T32-1	76	660	152	3	15.9	25.4	12.1	1044	25	23.4
		T32-2	76	660	152	3	15.9	25.4	12.0	1049	23	24.4
		T32-3	76	660	152	3	15.9	25.4	11.9	1022	10	32.5

⁽¹⁾Average value of the measured dimensions of the weld leg.

Table 2. Summary of the experimental results generated by testing lap joints with transverse fillet welds under axial loading (see also Figure 2).

Code	Ref.	Specimen code	w [mm]	l [mm]	p [mm]	g [mm]	t [mm]	T [mm]	s⁽¹⁾ [mm]	F_f [kN]	Error [%]
A	[9]	1-2-L-0	101.6	711.2	101.6	50.8	25.4	25.4	6.9	1099	15.7
		2-2-L-0	101.6	711.2	101.6	50.8	25.4	25.4	7.2	1081	12.7
		3-3-L-0	101.6	711.2	101.6	50.8	38.1	38.1	10.5	1495	26.2
		4-3-L-0	101.6	711.2	101.6	50.8	38.1	38.1	10.0	1477	25.8
		5-4-L-0	101.6	711.2	101.6	50.8	50.8	50.8	14.2	1566	12.1
		6-4-L-0	101.6	711.2	101.6	50.8	50.8	50.8	14.4	1691	20.7
C1	[33]	L1-1	95.3	609.6	50.8	0	31.8	31.8	10.3	731	-23.6
		L1-2	95.3	609.6	50.8	0	31.8	31.8	10.7	762	-22.2
		L1-3	95.3	609.6	50.8	0	31.8	31.8	10.5	740	-22.0
C2	[33]	L2-1	95.3	609.6	50.8	0	31.8	31.8	11.2	830	10.2
		L2-2	95.3	609.6	50.8	0	31.8	31.8	10.8	805	-10.6
		L2-3	95.3	609.6	50.8	0	31.8	31.8	11.0	802	-8.2
C3	[33]	L3-1	95.3	609.6	50.8	0	31.8	31.8	10.4	743	8.9
		L3-2	95.3	609.6	50.8	0	31.8	31.8	10.7	700	-5.1
		L3-3	95.3	609.6	50.8	0	31.8	31.8	10.5	750	0.7

⁽¹⁾Average value of the measured dimensions of the weld leg.

Table 3. Summary of the experimental results generated by testing longitudinal fillet welds under axial loading (see also Figure 4a).

Code	Ref.	Specimen code	w [mm]	l [mm]	p [mm]	g [mm]	m [mm]	t [mm]	T [mm]	s⁽¹⁾ [mm]	F_r [kN]	Error [%]
D1	[34]	TL50-1	152	917	51	3	76	44	44	13.1	1484	-9.5
		TL50-2	152	917	51	3	76	44	44	12.9	1664	2.4
		TL50-3	152	917	51	3	76	44	44	12.7	1573	-1.2
		TL50-4	152	917	51	3	76	44	44	13.3	1700	1.6
		TL50a-1	152	917	51	3	76	44	44	8.8	1299	3.5
		TL50a-2	152	917	51	3	76	44	44	9.2	1186	-8.9
		TL50a-3	152	917	51	3	76	44	44	9.0	1213	-4.1
		TL50a-4	152	917	51	3	76	44	44	9.8	1472	6.7
D2	[34]	TL100-1	152	1223	102	3	76	70	70	14.5	2359	2.5
		TL100-2	152	1223	102	3	76	70	70	13.2	2218	-4.5
		TL100-3	152	1223	102	3	76	70	70	13.1	1976	-9.2
		TL100SP-1	152	1223	102	3	76	70	70	11.3	2032	0.5
		TL100SP-2	152	1223	102	3	76	70	70	11.7	1866	-9.0
		TL100SP-3	152	1223	102	3	76	70	70	11.9	1813	-15.4
		TL100D-1	152	1223	102	3	76	70	70	12.1	2077	-2.7
		TL100D-2	152	1223	102	3	76	70	70	12.2	2040	-3.0
		TL100D-3	152	1223	102	3	76	70	70	14.0	2341	4.3
		TL50D-1	152	1223	51	3	76	51	51	13.7	1489	1.4
		TL50D-2	152	1223	51	3	76	51	51	13.5	1455	-3.4
		TL50D-3	152	1223	51	3	76	51	51	13.5	1412	-3.8

⁽¹⁾Average value of the measured dimensions of the weld leg.

Table 4. Summary of the experimental results generated by testing combined longitudinal and transverse fillet welds under axial loading (see also Figure 5a).

Code	Ref.	Specimen code	w [mm]	l [mm]	p [mm]	g [mm]	t [mm]	T [mm]	s⁽¹⁾ [mm]	F_f [kN]	Error [%]
E1	[33]	F1-1	54.0	816.0	152.4	3.2	25.4	50.8	11.2	789	5.0
		F1-2	54.0	816.0	152.4	3.2	25.4	50.8	10.0	763	8.5
		F1-3	54.0	816.0	152.4	3.2	25.4	50.8	10.3	745	6.9
E2	[33]	F2-1	54.0	816.0	152.4	3.2	25.4	50.8	10.2	813	21.8
		F2-2	54.0	816.0	152.4	3.2	25.4	50.8	10.8	840	21.1
		F2-3	54.0	816.0	152.4	3.2	25.4	50.8	10.6	823	23.6
E3	[33]	F3-1	54.0	816.0	152.4	3.2	25.4	50.8	11.6	755	35.3
		F3-2	54.0	816.0	152.4	3.2	25.4	50.8	10.5	725	33.8

⁽¹⁾Average value of the measured dimensions of the weld leg.

Table 5. Summary of the experimental results generated by testing inclined fillet welds under axial loading (see also Figure 6a)

Code	Ref.	Specimen code	T [mm]	l [mm]	w [mm]	e [mm]	s [mm]	F_f [kN]	Error [%]
		B_125_A516_55_1	32.1	508.0	101.6	139.7	10.1	197.6	-6.8
		B_125_A516_55_2	32.1	508.0	101.6	139.7	10.1	239.0	7.4
		B_125_A516_55_3	32.1	508.0	101.6	139.7	10.4	233.6	3.4
		B_125_A12_55_1	32.1	508.0	101.6	139.7	15.0	326.6	16.1
		B_125_A12_55_2	32.1	508.0	101.6	139.7	15.0	321.3	13.6
		B_125_A12_55_3	32.1	508.0	101.6	139.7	14.9	316.4	11.3
		B_175_A516_3_1	44.8	508.0	101.6	76.2	9.1	534.0	-10.2
		B_175_A516_3_2	44.8	508.0	101.6	76.2	9.3	529.6	-14.1
		B_175_A516_3_3	44.8	508.0	101.6	76.2	9.2	551.4	-4.6
		B_175_A12_3_1	44.8	508.0	101.6	76.2	14.0	682.6	1.5
		B_175_A12_3_2	44.8	508.0	101.6	76.2	14.1	778.8	-17.1
		B_175_A12_3_3	44.8	508.0	101.6	76.2	14.5	676.9	-8.9
		B_175_A516_55_1	44.8	508.0	101.6	139.7	9.3	274.6	-1.4
		B_175_A516_55_2	44.8	508.0	101.6	139.7	9.3	265.7	7.8
F1	[35]	B_175_A516_55_3	44.8	508.0	101.6	139.7	9.4	280.4	-3.8
		B_175_A12_55_1	44.8	508.0	101.6	139.7	15.2	400.5	15.7
		B_175_A12_55_2	44.8	508.0	101.6	139.7	14.3	340.9	11.5
		B_175_A12_55_3	44.8	508.0	101.6	139.7	14.8	354.2	8.5
		B_175_A516_85_1	44.8	508.0	101.6	215.9	10.6	173.6	11.8
		B_175_A516_85_2	44.8	508.0	101.6	215.9	10.7	134.0	3.2
		B_175_A516_85_3	44.8	508.0	101.6	215.9	10.6	148.6	6.3
		B_175_A12_85_1	44.8	508.0	101.6	215.9	14.9	231.0	-10.4
		B_175_A12_85_2	44.8	508.0	101.6	215.9	14.6	228.3	3.7
		B_175_A12_85_3	44.8	508.0	101.6	215.9	15.8	235.9	-5.4
		B_250_A516_55_1	64.2	508.0	101.6	139.7	10.3	275.9	-8.1
		B_250_A516_55_2	64.2	508.0	101.6	139.7	10.2	261.2	-3.2
		B_250_A516_55_3	64.2	508.0	101.6	139.7	10.1	259.4	-9.5
		B_250_A12_55_1	64.2	508.0	101.6	139.7	14.8	386.7	-4.6
		B_250_A12_55_2	64.2	508.0	101.6	139.7	14.6	452.1	5.8
		B_250_A12_55_3	64.2	508.0	101.6	139.7	14.1	420.5	24.7

Table 6 (caption on the next page).

Code	Ref.	Specimen code	T [mm]	l [mm]	w [mm]	e [mm]	s [mm]	F_f [kN]	Error [%]
		B_125_B516_55_1	32.4	508.0	101.6	139.7	10.8	224.7	6.0
		B_125_B516_55_2	32.4	508.0	101.6	139.7	10.8	255.4	16.8
		B_125_B516_55_3	32.4	508.0	101.6	139.7	10.7	270.6	30.2
		B_125_B12_55_1	32.4	508.0	101.6	139.7	15.0	364.9	7.6
		B_125_B12_55_2	32.4	508.0	101.6	139.7	14.3	376.0	14.6
		B_125_B12_55_3	32.4	508.0	101.6	139.7	15.4	439.7	16.9
		B_175_B516_3_1	45.1	508.0	101.6	76.2	10.2	735.1	-1.2
		B_175_B516_3_2	45.1	508.0	101.6	76.2	9.7	713.8	5.5
		B_175_B516_3_3	45.1	508.0	101.6	76.2	9.8	691.1	8.4
		B_175_B12_3_1	45.1	508.0	101.6	76.2	14.8	859.7	12.5
		B_175_B12_3_2	45.1	508.0	101.6	76.2	14.7	890.0	16.4
		B_175_B12_3_3	45.1	508.0	101.6	76.2	14.3	825.0	10.8
		B_175_B516_55_1	45.1	508.0	101.6	139.7	11.3	385.8	12.5
		B_175_B516_55_2	45.1	508.0	101.6	139.7	10.8	310.6	17.2
F2	[35]	B_175_B516_55_3	45.1	508.0	101.6	139.7	9.1	347.1	22.2
		B_175_B12_55_1	45.1	508.0	101.6	139.7	14.8	441.9	7.3
		B_175_B12_55_2	45.1	508.0	101.6	139.7	15.3	400.5	6.8
		B_175_B12_55_3	45.1	508.0	101.6	139.7	14.6	385.4	7.7
		B_175_B516_85_1	45.1	508.0	101.6	215.9	10.6	204.3	15.0
		B_175_B516_85_2	45.1	508.0	101.6	215.9	10.6	208.3	13.8
		B_175_B516_85_3	45.1	508.0	101.6	215.9	10.6	204.7	14.0
		B_175_B12_85_1	45.1	508.0	101.6	215.9	14.9	263.9	-6.5
		B_175_B12_85_2	45.1	508.0	101.6	215.9	15.3	266.6	-7.3
		B_175_B12_85_3	45.1	508.0	101.6	215.9	16.0	254.1	1.8
		B_250_B516_55_1	64.5	508.0	101.6	139.7	9.7	346.7	15.2
		B_250_B516_55_2	64.5	508.0	101.6	139.7	10.1	342.7	10.5
		B_250_B516_55_3	64.5	508.0	101.6	139.7	10.3	340.0	10.0
		B_250_B12_55_1	64.5	508.0	101.6	139.7	15.8	491.7	3.0
		B_250_B12_55_2	64.5	508.0	101.6	139.7	16.3	498.4	6.5
		B_250_B12_55_3	64.5	508.0	101.6	139.7	15.6	492.6	9.2

Table 6. Summary of the experimental results generated by testing cruciform welded joints under out-of-plane three-point bending (see also Figure 7a).

Code	Specimen code	Ref.	Geometry	Error [%] – Eq. (10)		
				<i>Point Method</i>	<i>Directional Method</i>	<i>Simplified Method</i>
A	7-2-T-0	[9]	Fig. 2a	-1.2	7.9	32.2
A	1-2-L-0	[9]	Fig. 4a	15.7	1.6	1.8
D1	TL50-1	[34]	Fig. 5a	-9.5	21.4	33.7
E1	F1-1	[33]	Fig. 6a	5	70.4	86.5
F1	B_125_A516_55_1	[35]	Fig. 7a	-7.7	-9.5	54.8

Table 7. Accuracy of the Point Method, Directional Method [15], and Simplified Method [15] in estimating the static strength of steel arc welded joints.

Figures

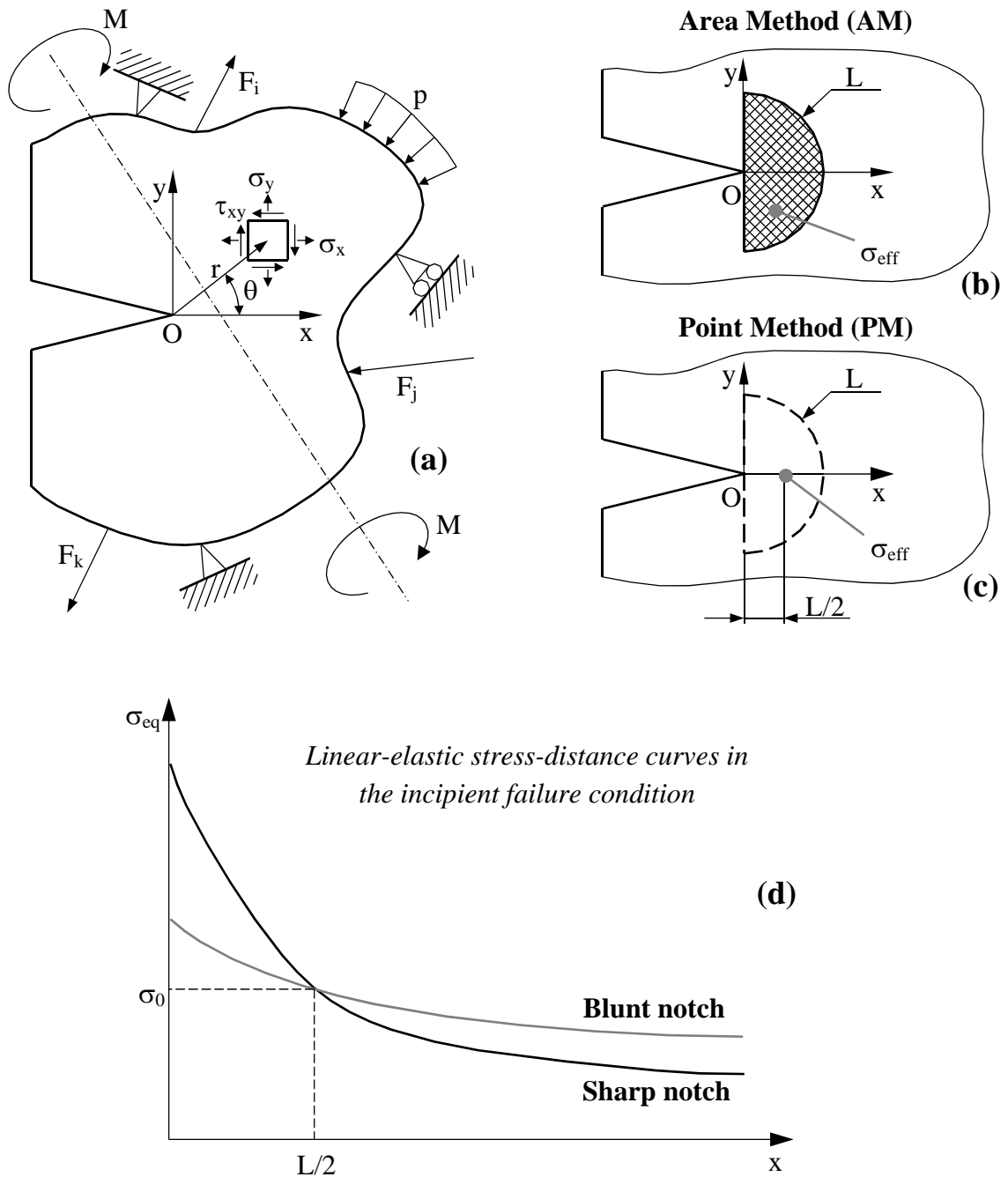


Figure 1. Notched component subjected to a complex system of external forces/ moments and local system of coordinates (a); effective stress calculated according to the Area (b) and to the Point Method (c); Determination of inherent strength σ_0 and critical distance L via experimental results generated by testing notches of different sharpness (d).

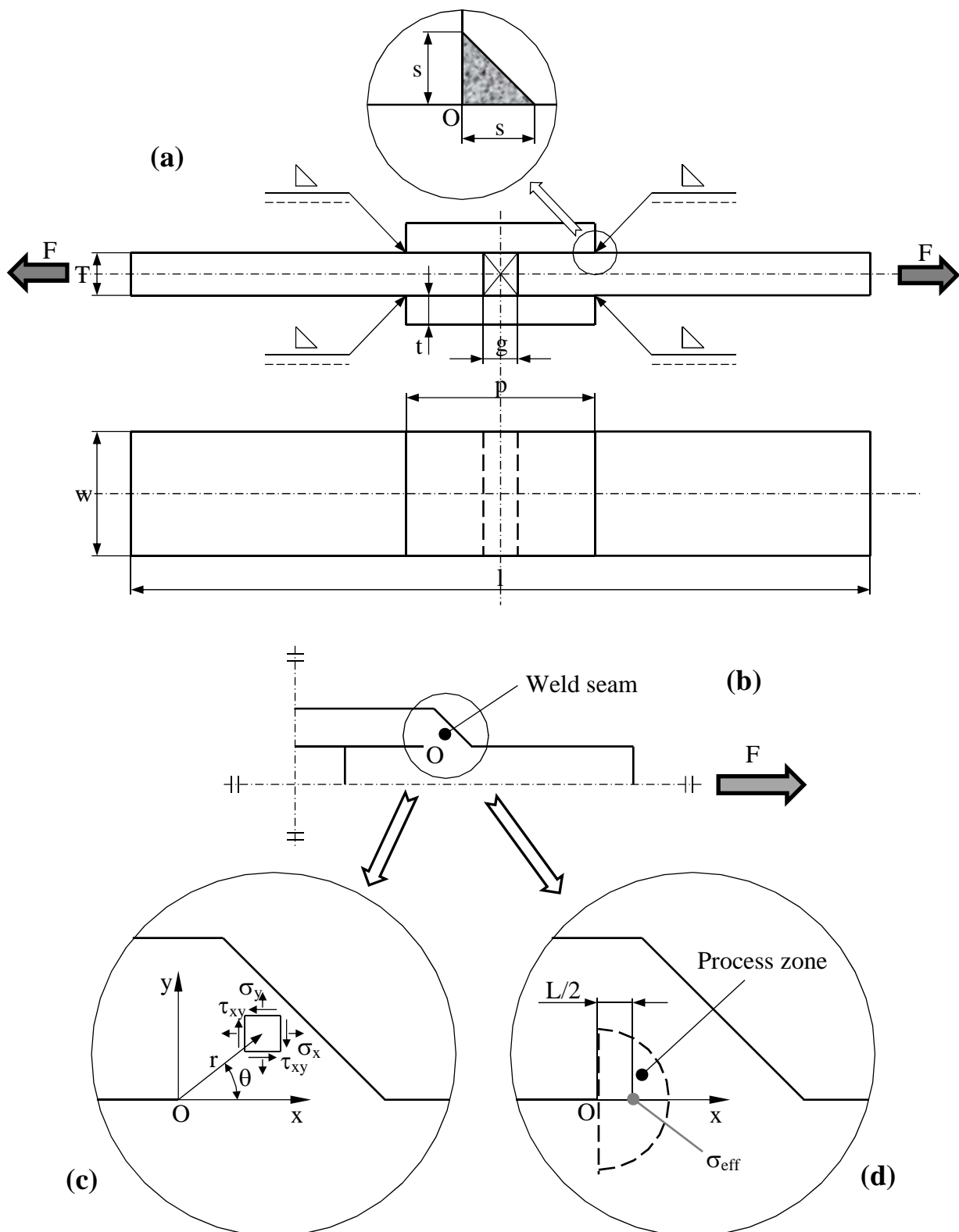
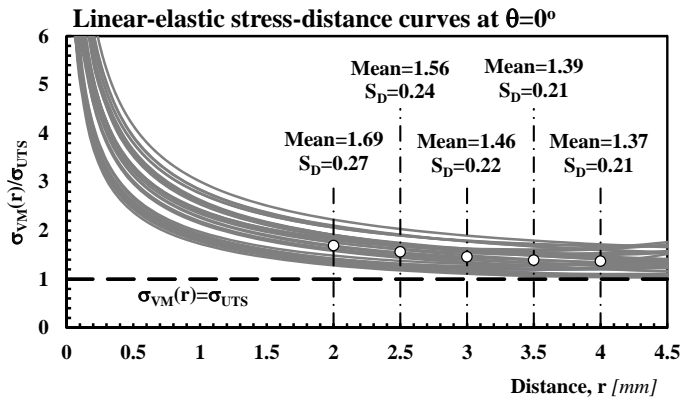
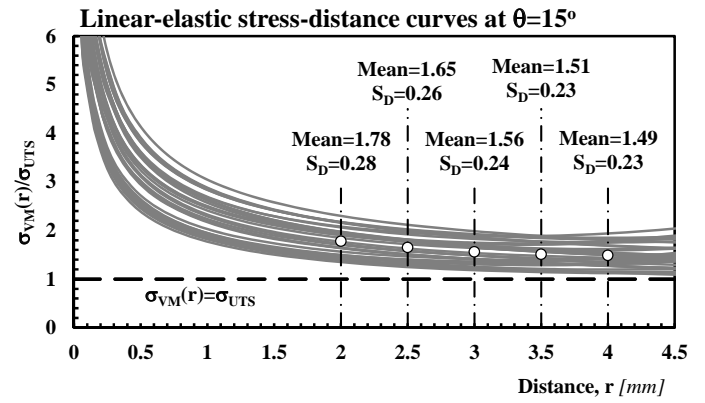


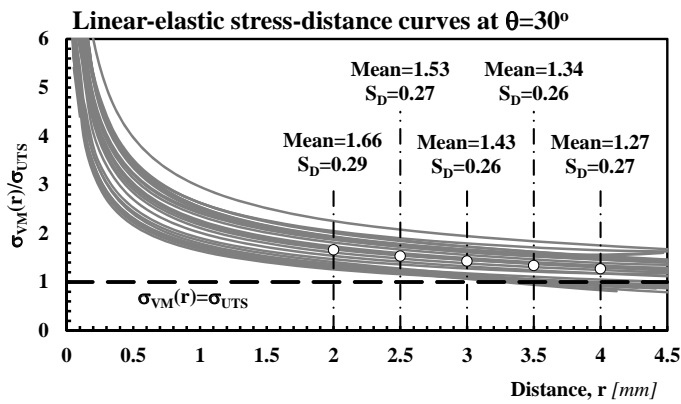
Figure 2. Lap joint with transverse fillet welds: technical drawing (a), simplified reference geometry (b), local system of coordinates centred at the tip of the crack-like notch (c), effective stress determined according to the PM (d).



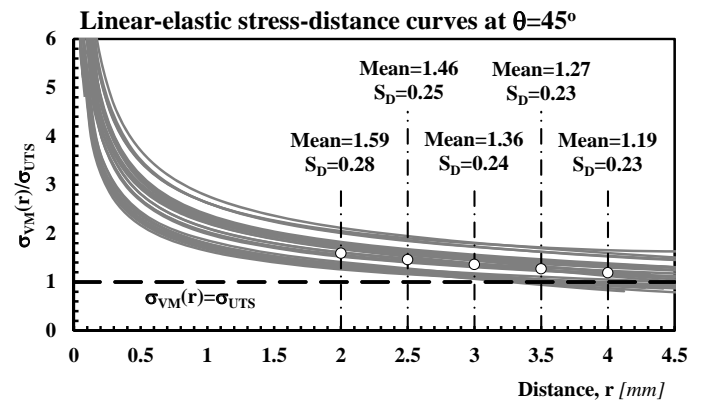
(a)



(b)

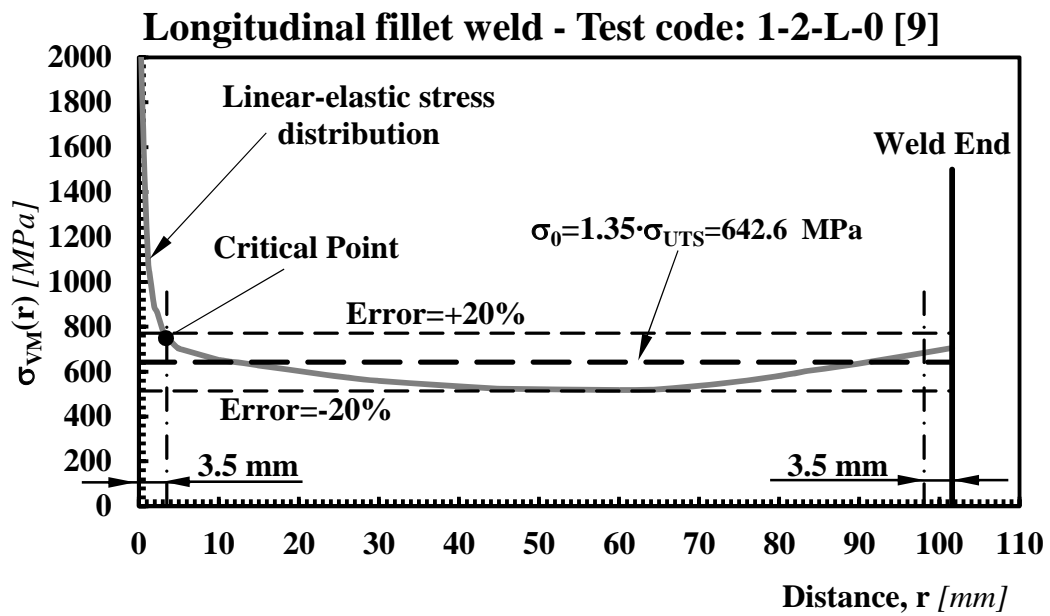
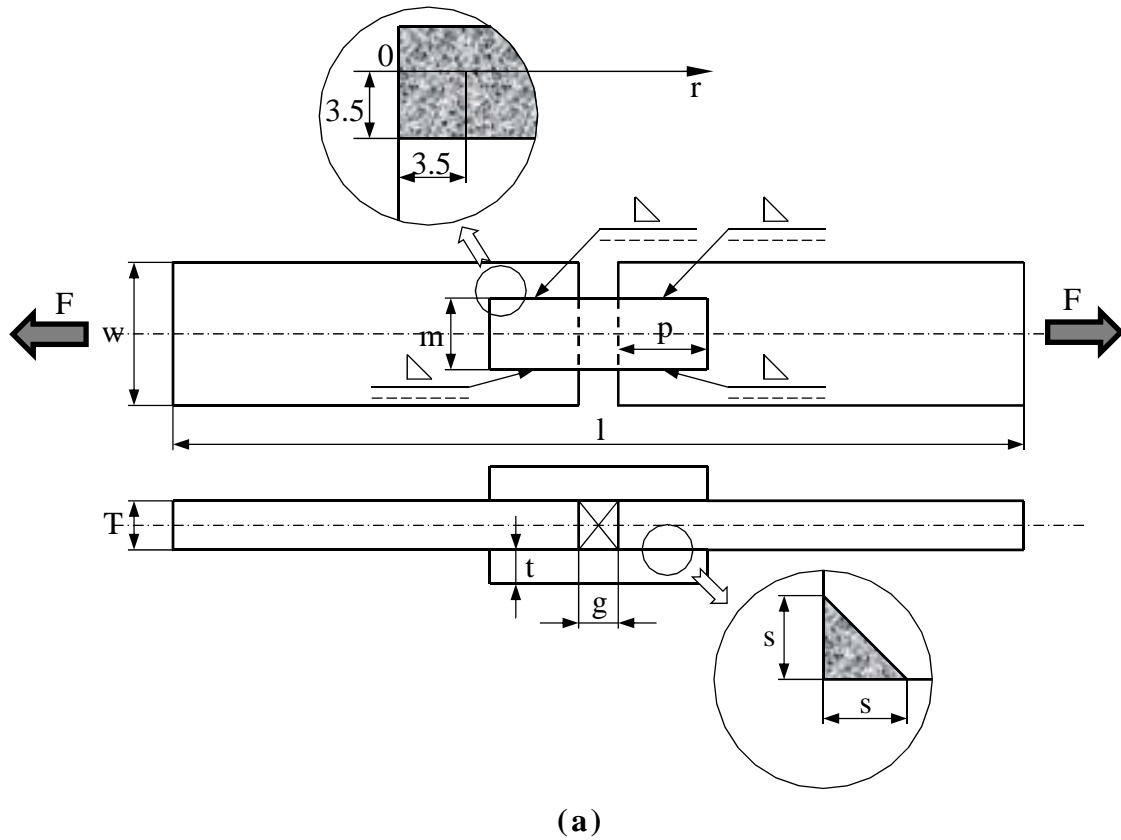


(c)



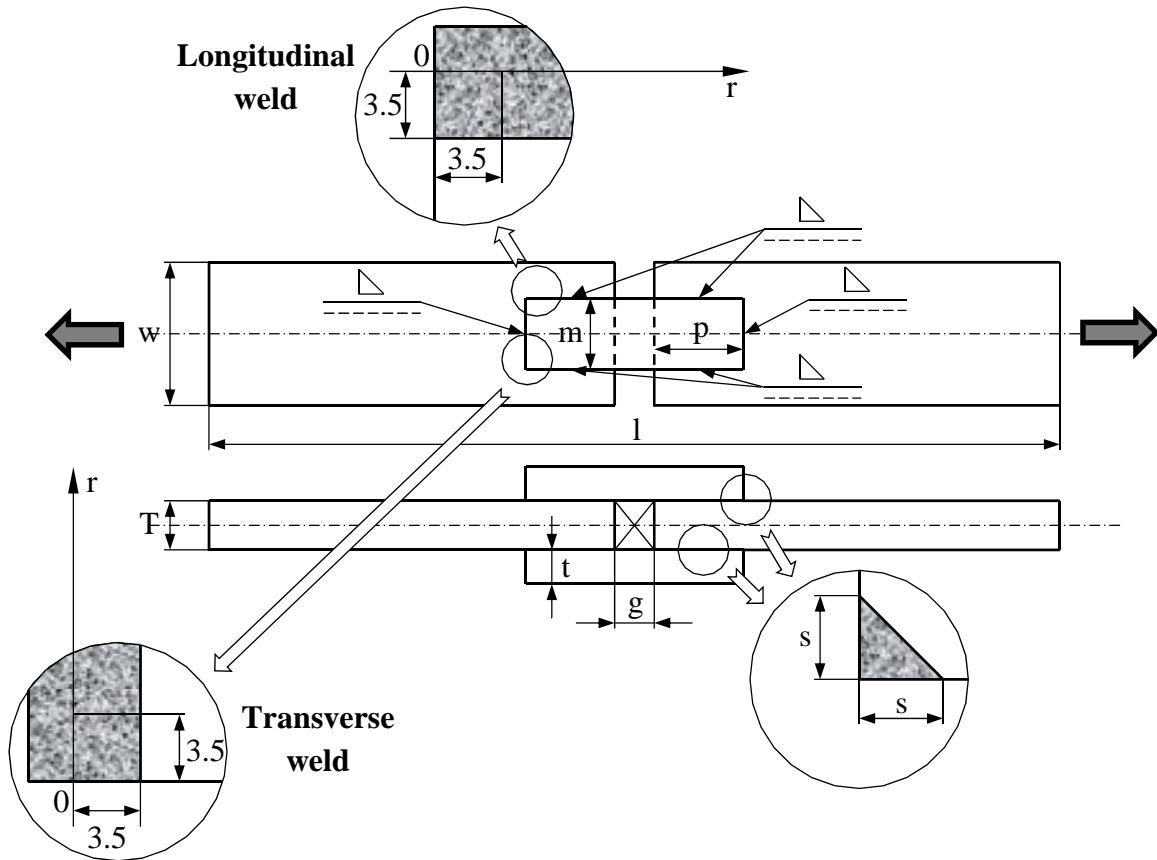
(d)

Figure 3. Linear-elastic stress-distance curves plotted, in the incipient failure condition, at different values of angle θ for lap joints with transverse fillet welds (see Figure 2 and Table 2).

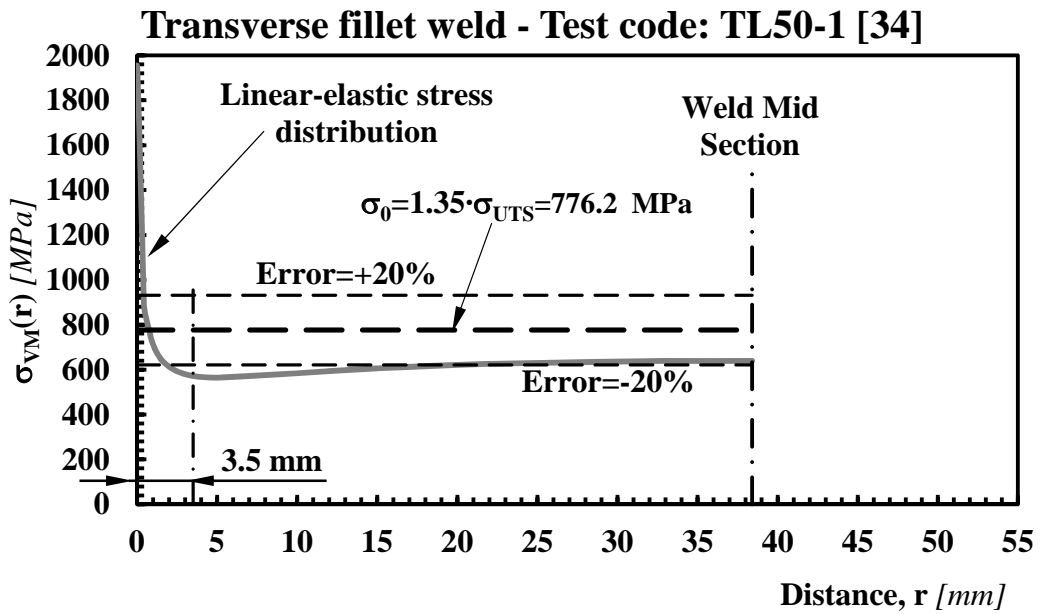


(b)

Figure 4. Longitudinal fillet weld specimens (a) and linear elastic stress distribution, in the incipient failure condition, along the weld seam for test 1-2-L-0 [9] (b) – see also Table 3.



(a)



(b)

Figure 5 (Contin.)

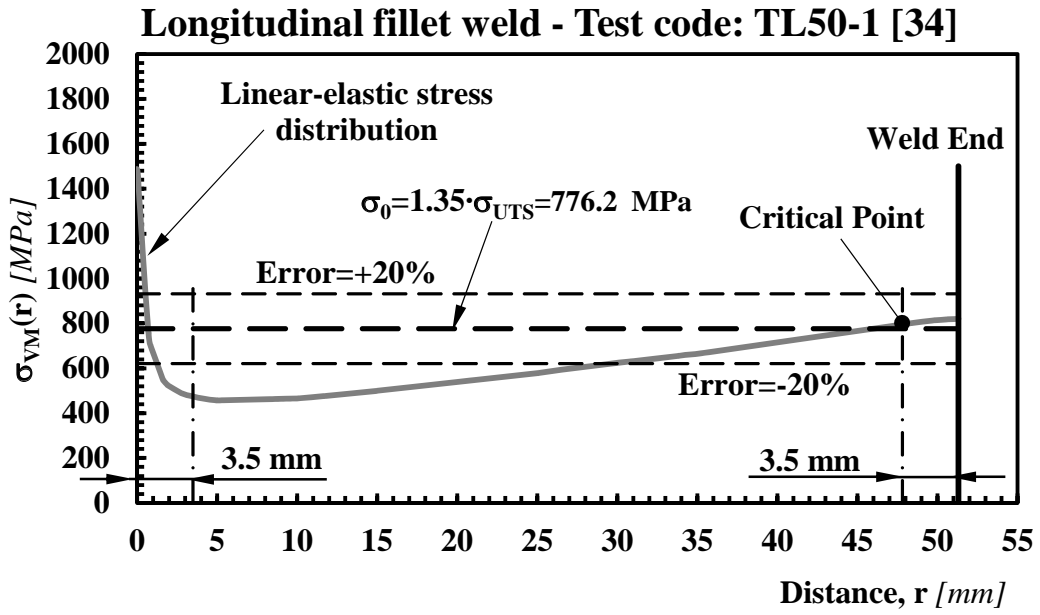
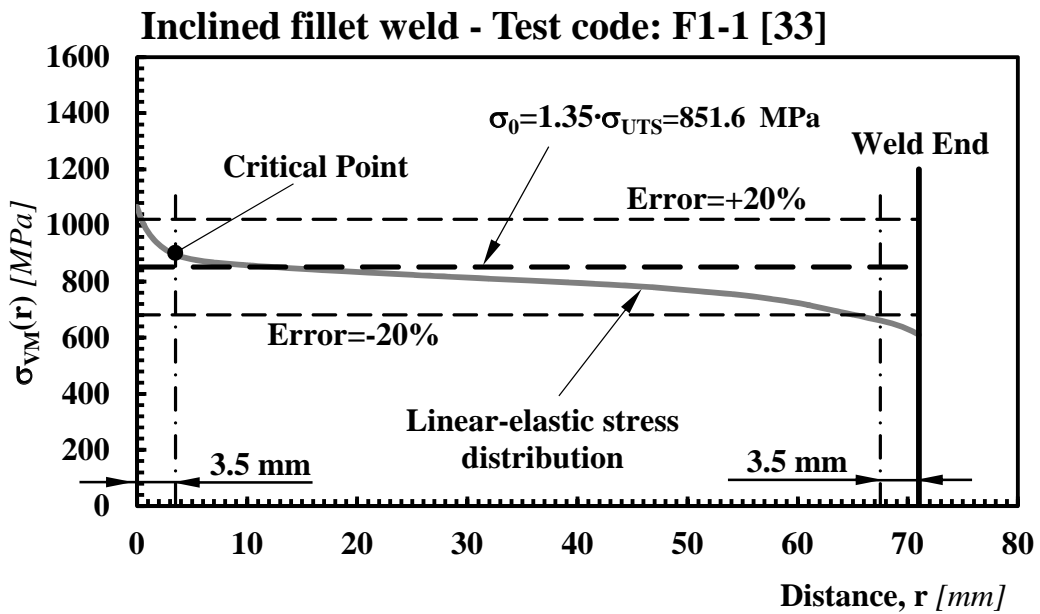
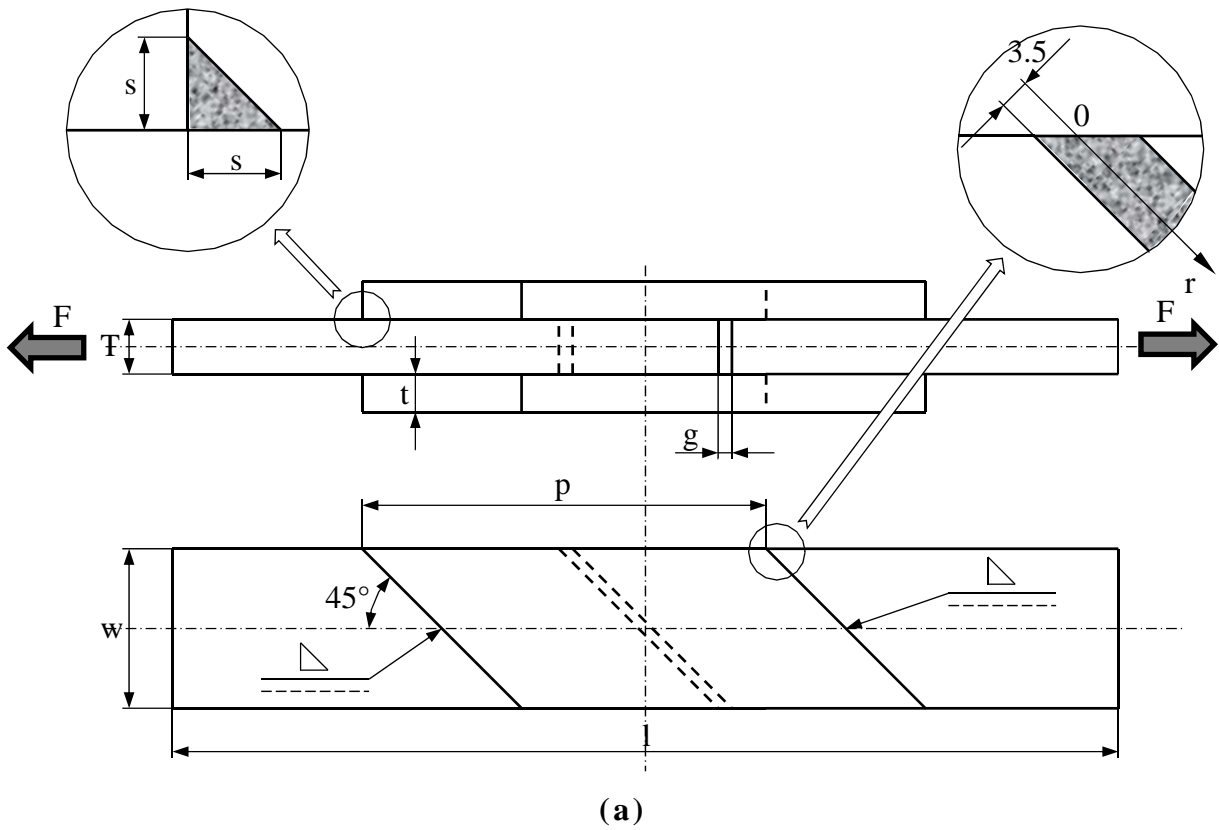


Figure 5. Combined longitudinal and transverse fillet weld specimens (a); linear elastic stress distribution, in the incipient failure condition, along the transverse (b) and the longitudinal (c) weld seam for test TL50-1 [34] (see Table 4).



(b)

Figure 6. Inclined fillet weld specimens (a); linear elastic stress distribution, in the incipient failure condition, along the weld seam for test F1-1 [33] (b) – see also Table 5.

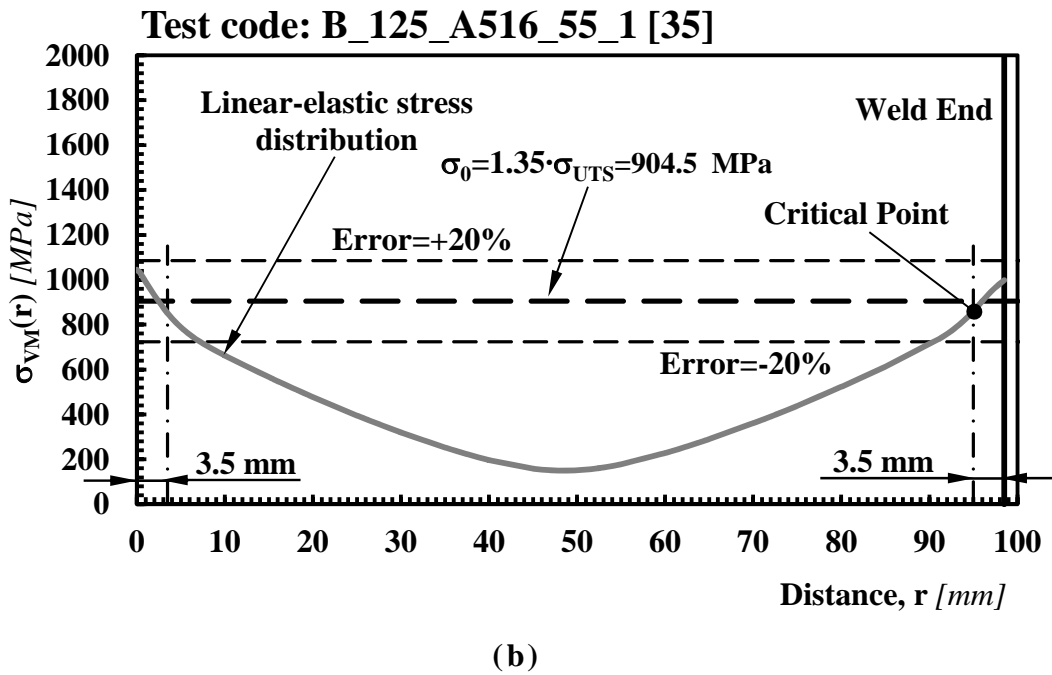
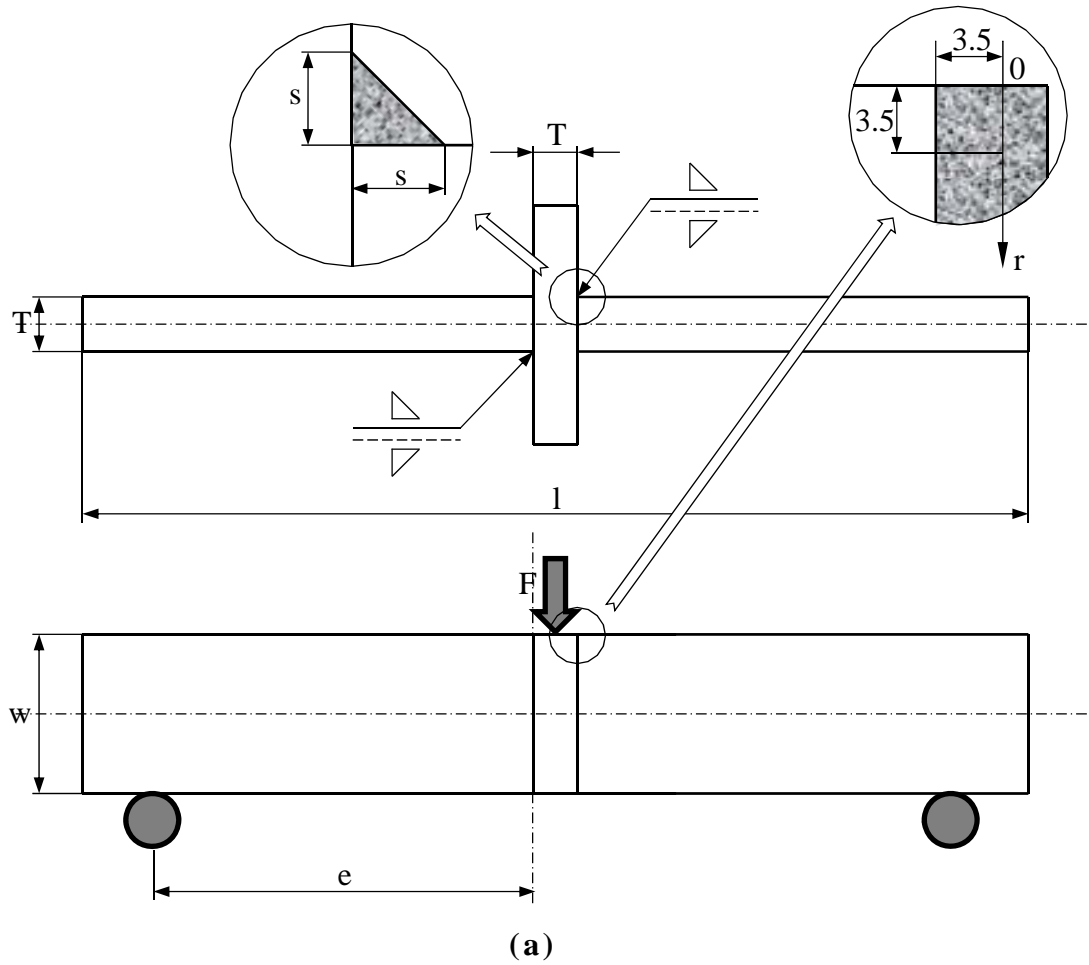
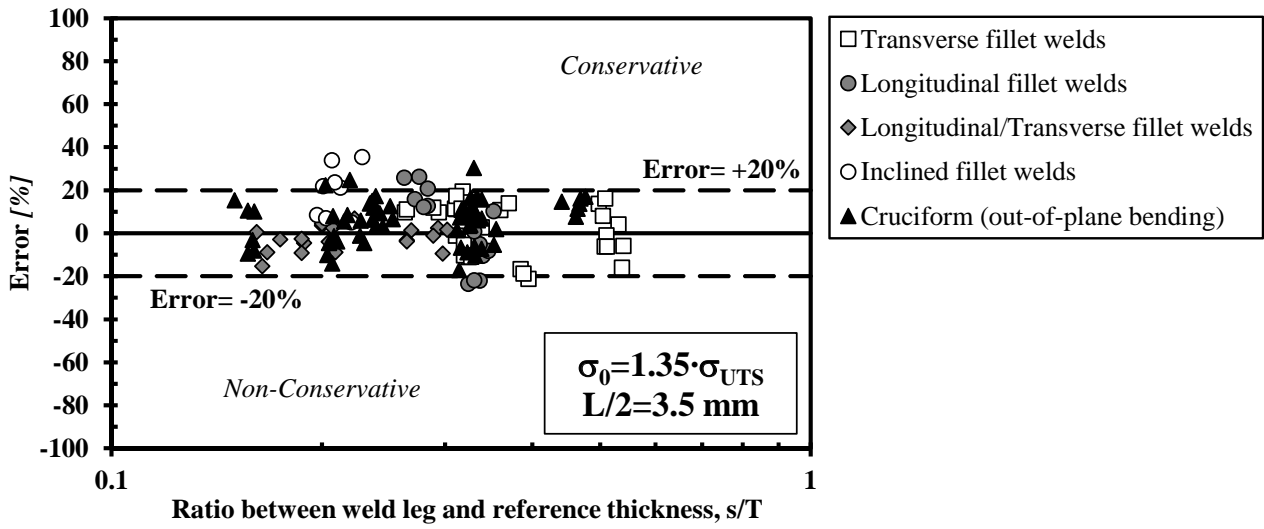
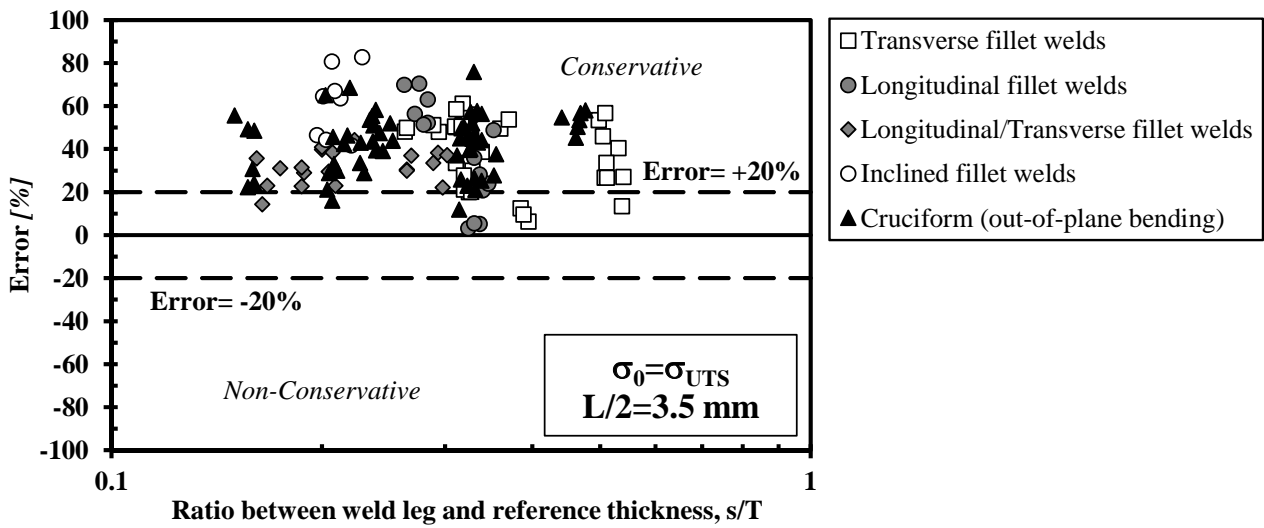


Figure 7. Cruciform welded joints loaded in out-of-plane three-point bending (a); linear elastic stress distribution, in the incipient failure condition, along the weld seam for test B_125_A516_55_1 [35] (b) - see also Table 6.



(a)



(b)

Figure 8. Overall accuracy of the proposed approach obtained by taking $\sigma_0 = 1.35 \cdot \sigma_{UTS}$ (a) and $\sigma_0 = \sigma_{UTS}$ (b).